| Title | フェージング環境における周波数変調通信方式の検波特性に関する研究 |
| --- | --- |
| Author(s) | 樫木, 勘四郎 |
| Citation | 大阪大学, 1981, 博士論文 |
| Version Type | VoR |
| URL | https://hdl.handle.net/11094/1907 |
| rights | |
| Note | |

# DETECTION CHARACTERISTICS

# OF FREQUENCY MODULATION SYSTEMS

# IN FADING ENVIRONMENTS

KANSHIROH KASHIKI

JANUARY 1981

20

To my parents

# DETECTION CHARACTERISTICS

# OF FREQUENCY MODULATION SYSTEMS

# IN FADING ENVIRONMENTS

（フェージング環境における周波数変調通信方式の検波特
性に関する研究）

## KANSHIROH  KASHIKI

樫　　木　　勘四郎

JANUARY  1981

# Acknowledgements

# Preface

This thesis investigates the detection characteristics of analog frequency modulation system, digital frequency modulation system, and digital phase-frequency modulation system, in fading environments.

It consists of eight chapters described as follows:

Chapter 1 presents a review of previous and recent researches on frequency modulation systems concerned in this thesis, and gives the significance and the originality of this study.

Chapter 2 gives a basic analysis for the output characteristics of analog frequency modulation system employing a conventional limiter-discriminator detector. Expressions are given for three kinds of power; signal, random noise, and click noise. Finally the output Signal-to-Noise power Ratio (SNR) is defined.

Chapter 3 investigates the output SNR and the noise characteristics of the analog frequency modulation system in the nonselective $m$-distributed fading environments, and the improvement effects on the output SNR performance by the predetection diversity techniques; Selection Combining (SC), Equal-Gain Combining (EGC), and Maximal-Ratio Combining (MRC). Degradation characteristics due to the correlation between two diversity branches are also taken into account. Average number of clicks, power ratio of click noise to random noise, and output SNR are graphically presented as functions of input Carrier-to-Noise power Ratio (CNR) and fading figure. A comparison for the types of the diversity techniques is made and

a design method for the frequency modulated TV signal transmission is given as an example.

Chapter 4 gives a basic analysis for the error rate characteristics of the digital frequency modulation system employing a limiter-discriminator with an integrate-and-dump filter. Expressions are given for the probability density function of the integrate-and-dump filter output and for the error rate.

Chapter 5 investigates the error rate characteristics of the digital frequency modulation system in the nonselective $m$-distributed fading environments, the improvement effects by the predetection or the postdetection diversity techniques, and the degradation characteristics due to the correlation between two diversity branches. In the case of the Switch-and-Stay diversity, an optimum switching level attaining the minimum error rate is derived. The results are given in graphs showing the relationship among the error rate, input CNR, modulation index, and fading figure, and a comparison is made for the types of the diversity techniques. It is also shown that the optimum modulation index giving the minimum attainable error rate is not to be affected by the fading figure, input CNR, and type of diversity technique, except for the postdetection diversity.

Chapter 6 proposes a new phase-frequency modulation system and discusses its noncoherent detection systems. It is shown that the derived error rate becomes the same as that of DPSK system.

Chapter 7 investigates the error rate characteristics of the proposed phase-frequency modulation system in the nonselective $m$-distributed fading or the time-selective Rayleigh fading environments. The results obtained show that the Doppler phenomenon affects more strongly the error rate of the phase information than that of the frequency information.

Chapter 8 summarizes the results obtained in this thesis.

# Table of Contents

# List of Figures

Chapter 1

INTRODUCTION

One of the basic problems of communication engineering
is the design and analysis of systems which transmit various
types of information with maximum accuracy and efficiency.
To achieve this object, many investigators have been engaged
in the research and development on various kinds of communi-
cation system, whose evaluations are based on the output
Signal-to-Noise power Ratio (SNR) for analog systems and the
error rate for digital systems [1]-[6]. Analog communication
systems include Amplitude Modulation (AM), Phase Modulation
(PM), and Frequency Modulation (FM). This class of systems
has an advantage of simple implementation of the detection
systems. However, the recent hasty progress in digital
techniques requires reliable digital communication systems,
which include digital AM (ASK: Amplitude Shift Keying),
digital PM (PSK: Phase Shift Keying), and digital FM (FSK:
Frequency Shift Keying).

## 1.1 Scope of This Work

The well-known analog FM systems have been applied to
the transmission of audio signal such as the commercial
stereo broadcasting and of image signal such as the televi-
sion signal through the satellite [7], while digital FM sys-
tems have been applied to space communications [8] and mobile
paging systems [9]. The advantage of both analog and digital
FM systems is their simple implementation by the employment
of a conventional limiter-discriminator and their smaller

performance degradation caused by a nonlinear device such as the travelling wave tube (TWT) [5].

Concerning digital modulation systems, although there has been a large literature discussing the performance of basic systems such as ASK, PSK, and FSK, the increasing demand for data transmission with limited bandwidth has borne the so-called hybrid modulation, which includes QAM (Quadrature Amplitude Modulation) system [10] using the combination of amplitude and phase keying. However, if this signal passes through a TWT operating in the saturation region, the amplitude information will be lost.

In this thesis, a new hybrid modulation named "digital phase-frequency modulation " is thus proposed and its output performance is discussed when noncoherently detected. This new system bears information in the phase and the frequency domains, so that the information is deemed not to be lost in such a system using the TWT as mentioned above.

Fading phenomenon is an important degradation factor in addition to input noise or RF interferences [11]-[16]. When the signal is transmitted through a steady media such as line-of-sight path, fading is not induced. However, over the ionosphere, troposphere, and urban radio channels, the transmitted signal will be subject to fading. For these motivations, the performance of three kinds of communication system are analyzed in fading environments.

## 1.2 Relation between This Work and Previous Work
### 1.2.1 Fading Model

In the literatures up to the present, almost all the fading models have assumed either the Rayleigh or the Rician distributions [17]-[21]. However, considering that the radio channels are being set up on the various modes of propagation

media and that millimeter wave systems are being
developed, the fading model to be assumed is necessary to
represent a wide class of fading, ranging from deep to shallow
fading. This motivation leads to the adoption of the m-distri-
bution formulated by Nakagami [22], which has a parameter $m$
as a fading figure showing the degree of fading. In this
thesis, the detection characteristics of the three FM systems
are discussed in the $m$-distributed and nonselective fading
environments. The latter assumption means that the fading
rate is sufficiently small compared with the modulating signal
frequency and that any distortion to the signal is not induced
by the fading channel.

In the application to the urban radio channels [23],
especially in UHF or microwave radio channels, the signal is
subject to time-selective fading, which is caused by the re-
flection from and diffraction around buildings and terrain
when a vehicle is moving around, and Doppler phenomenon
becomes an important degradation factor. The previous analy-
ses of detection performance in such a fading environment
have been confined to the case of digital PM [24] and digital
FM [25]-[26]. In this thesis, for the digital phase-frequency
modulation system, the effect of this type of fading is
discussed.

## 1.2.2  Diversity Technique

The diversity techniques are well-known to combat the
effect of fading and are classified into two kinds: the pre-
detection diversity and postdetection diversity. The former
has the combiner before the detector and the latter after the
detector. Typical predetection diversity techniques include
linear combining methods such as Switching, Selection Com-
bining (SC), Equal-Gain Combining (EGC), Maximal-Ratio Com-

bining (MRC) [27]. These types of diversity improve the output performance by reducing the percentage falling into the lower signal envelope level. However, the necessity to have the knowledge on the status of fading makes the combiner circuit complex, and if the knowledge is imperfect, the improvement effect degrades [28]. On the other hand, in the case of postdetection diversity, the unnecessity of such a knowledge makes the implementation simple.

In discussing the improvement effect by the diversity technique, one of the important factors is a correlation between two diversity branches. When two antennas are sufficiently separated, no correlation will occur. However, when the antenna spacing is limited as in the case of vehicles, the correlation will occur more or less, and the improvement effect will be degraded.

Although many analyses on the improvement effects by these diversity techniques have been reported [29], the analysis including the effect of correlation [30] and the comparison of predetection diversity and postdetection diversity are found only in a small literature.   Therefore, under the assumption that two branches are correlated, this thesis describes the diversity improvement effects on output SNR and noise characteristic for analog FM and on error rate for digital FM.  In addition, in the case of digital FM, the error rate analysis for predetection diversity and postdetection diversity clarifies the difference of improvement characteristics of two techniques.

## 1.3  Analysis Method

For the analog FM and the digital FM systems, this thesis adopts Rice's procedure [31],by which the output noise can be separated into the Gaussian random noise and the im-

pulsive click noise [32]-[33].

In the application of the analog FM system to the mono-chrome TV signal transmission, above the threshold region the picture appears grainy because of the random noise. However, below and around the threshold region the character of noise on the picture changes to include impulsive noise [34] and this noise appears as black and white dots with the black dots predominating in the white areas and the white dots predominating in the black areas. Therefore, the number of these dots becomes a basic evaluation of the output per-formance. Following Rice's procedure, it is possible to calculate the number of these dots per second.

In the analysis of the digital FM when detected by a conventional limiter-discriminator, early investigators have neglected the postdetection filter [35]-[36] or have assumed the performance at high input Carrier-to-Noise power Ratio (CNR) thus neglecting the threshold effect [37]. Although the distribution of instantaneous frequency for signal plus noise at the output of the discriminator is given [38]-[39], the result is not useful when the postdetection filter is employed, because there is no known relationship between the distributions before and after the postdetection filter [40]. On the other hand, the adoption of the concept of clicks extends the analysis to the case including the postdetection filter. In this thesis, when the postdetection filter is assumed to be an integrate-and-dump filter, the error rate is derived by the utilization of the probability density function of composite output of the desired signal, random noise, and click noise.

# Chapter 2

## ANALOG FREQUENCY MODULATION SYSTEM

## 2.1  Introductory Remark

In this chapter, descriptions are given for the detection
system of the analog Frequency Modulation (analog FM) signal,
which employs a conventional limiter-discriminator followed
by a low-pass filter, and for mathematical representation of
input and output components of the system.  The output compo-
nents consist of the desired signal, the continuous random noise,
and the impulsive click noise. Finally, the output Signal-to-
Noise power Ratio (SNR) is defined by the above three compo-
nents.

## 2.2  Analysis Model

The system under consideration is an analog FM detection
system employing a conventional limiter-discriminator.  As
shown in Fig. 2.1, the received analog FM signal is corrupted
by white Gaussian noise, passed through a band-pass filter
(BPF) at the carrier frequency $f_0$ with bandwidth $2B$, and sub-
sequently detected by the limiter-discriminator with a low-
pass filter.

The input analog FM signal $s(t)$ is defined by

$$s(t) = r\cos[\omega_0 t + \psi(t) + \theta] ,$$

(2.1)
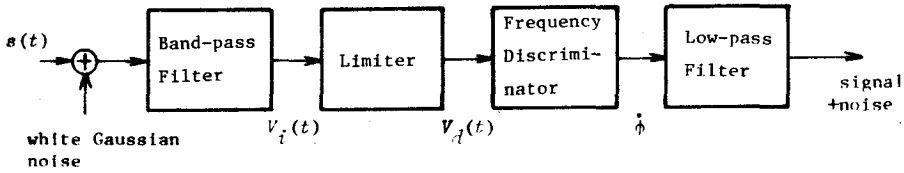
Fig. 2.1   Detection System for Analog

Frequency Modulation Signal.

where $r$ is the carrier envelope, $\omega_0 (=2\pi f_0)$ is the carrier angular frequency, $\dot{\psi}(t)$ $(=d\psi(t)/dt)$ is the modulating signal, and $\theta$ is the arbitrary phase of the carrier.

The input noise to the limiter, $n(t)$, is given by

$$n(t)=q(t)\cos[\omega_0 t+\lambda(t)] , \tag{2.2}$$

where $q(t)$ is the Rayleigh distributed envelope and $\lambda(t)$ is the uniformly distributed phase of the input noise.  An alternative expression may be represented by

$$n(t)=\xi(t)\cos\omega_0 t-\eta(t)\sin\omega_0 t , \tag{2.3}$$

where $\eta$ and $\xi$ are the quadrature and inphase components of the input noise with respect to the carrier frequency, and are uncorrelated Gaussian random processes of zero mean value and of variance $\sigma_n^2$.

The corrupted signal to the limiter, $V_i(t)$, can be written as

$$V_i(t) = r\cos[\omega_o t + \psi(t) + \theta] + q(t)\cos[\omega_o t + \lambda(t)]$$
$$= A(t)\cos[\omega_o t + \phi(t)] \ . \tag{2.4}$$

Referring to Fig. 2.2, the expressions for $A(t)$ and $\phi(t)$ become

$$A = \sqrt{\{r + q\cos(\lambda - \psi - \theta)\}^2 + \{q\sin(\lambda - \psi - \theta)\}^2} \tag{2.5}$$

$$\phi = \psi + \theta + \tan^{-1}\frac{q\sin(\lambda - \psi - \theta)}{r + q\cos(\lambda - \psi - \theta)} \ . \tag{2.6}$$
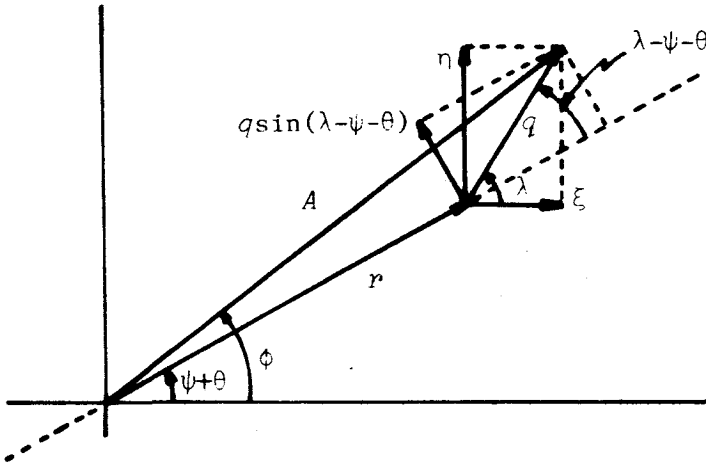


Fig. 2.2  Vector Diagram of Input Signal and Noise.

The limiter is used to suppress the envelope fluctuation of the corrupted input signal; therefore, the output $V_d(t)$ becomes ( $A(t)$ is normalized to 1 )

$$V_d(t) = \cos[\omega_o t + \phi(t)] \ . \tag{2.7}$$

Following the procedure of Rice [31] yields the approximate expression of (2.6)

$$\phi \approx \psi + \theta + \frac{q\sin(\lambda - \psi - \theta)}{r} \overset{\Delta}{=} \phi_k \ , \tag{2.8}$$

which becomes exact when $q \ll r$. In addition, considering the effects of the click noise peculiar to FM detection, the output of the frequency discriminator can be expressed as follows:

$$\dot{\phi} \approx \dot{\phi}_k + 2\pi(Z_+ - Z_-)$$

$$= \dot{\psi} + \dot{\theta} + \dot{y} + 2\pi\left\{\sum_{k=-\infty}^{\infty} \delta(t - t_k) - \sum_{l=-\infty}^{\infty} \delta(t - t_l)\right\} \ . \tag{2.9}$$

$$\left\{ \begin{array}{l} Z_+ = \displaystyle\sum_{k=-\infty}^{\infty} \delta(t - t_k) \\[2em] Z_- = \displaystyle\sum_{l=-\infty}^{\infty} \delta(t - t_l) \end{array} \right.$$

In the above equation, $\delta(\cdot)$ is the delta function, and $2\pi(Z_+ - Z_-)$ represents an additional factor necessary to account for the positive and negative clicks, which are impulsive. The term $\dot{y}$ represents the continuous random Gaussian noise as expressed below.

$$\left. \begin{array}{l} \dot{y}(t) = \dfrac{dy(t)}{dt} \\[2em] y = \dfrac{q\sin(\lambda - \psi - \theta)}{r} = \dfrac{\eta\cos(\psi + \theta) - \xi\sin(\psi + \theta)}{r} \end{array} \right\} \tag{2.10}$$

$$\eta = q\sin\lambda \qquad \xi = q\cos\lambda \ . \tag{2.11}$$

It is worth noting that $y$ is the ratio of the quadrature noise component (with respect to the input signal) to the envelope of the input signal.

## 2.3 Autocorrelation Function of Frequency Discriminator Output

Since $\dot{\phi}_k$ and $2\pi(Z_+-Z_-)$ are independent of each other, the autocorrelation function of $\dot{\phi}$, $R_{\dot{\phi}}(\tau)$, can be expressed as

$$R_{\dot{\phi}}(\tau)=R_{\dot{\phi}_k}(\tau)+R_{Z\pm}(\tau) ,$$  (2.12)

where the first term $R_{\dot{\phi}_k}(\tau)$ is the autocorrelation

function of $\dot{\phi}_k$ and the second term $R_{Z\pm}(\tau)$ is that of $2\pi(Z_+-Z_-)$. Because $\dot{\psi}$, $\dot{\theta}$, and $\dot{y}$ are independent of each other, the autocorrelation function $R_{\dot{\phi}_k}(\tau)$ can be resolved into three components:

$$R_{\dot{\phi}_k}(\tau)=R_{\dot{\psi}}(\tau)+R_{\dot{\theta}}(\tau)+R_{\dot{y}}(\tau) .$$  (2.13)

The phase $\theta$ is regarded as constant now; therefore the effect of $R_{\dot{\theta}}(\tau)$ in (2.13) can be neglected and $R_{\dot{\phi}}(\tau)$ becomes

$$R_{\dot{\phi}}(\tau)=R_{\dot{\psi}}(\tau)+R_{Z\pm}(\tau)+R_{\dot{y}}(\tau) .$$  (2.14)

This equation shows that the output autocorrelation function becomes a linear sum of $R_{\dot{\psi}}(\tau)$, $R_{Z\pm}(\tau)$, and $R_{\dot{y}}(\tau)$.

## 2.4 Output Signal Power

In this analysis, it is assumed that the modulation signal $\dot{\psi}(t)$ is a stationary Gaussian random process and its maximum frequency is $f_m$ Hz. Then, the output signal power $S_O$ is defined as

$$S_O=R_{\dot{\psi}}(0)=E[\dot{\psi}^2]=(2\pi\Delta f)^2 ,$$  (2.15)

where $\Delta f$ is the r.m.s. (root mean square) frequency deviation and $E[\cdot]$ denotes the ensemble average operation.

The modulation index $\beta$ is defined as

$$\beta = \frac{\Delta f}{f_m} \quad , \tag{2.16}$$

and the bandwidth of the bandpass filter is defined as

$$2B = 4\Delta f = 4\beta f_m \quad , \tag{2.17}$$

for passing the input analog FM signal without distortion.

## 2.5  Output Noise Power
### 2.5.1  Click Noise Power

The $Z_+$, $Z_-$ processes are sums of positive and negative impulses (as shown in (2.9)), which occur at random times and are assumed to be independent of one another. Furthermore, they follow the Poisson process with average number of $N_+$ and $N_-$ [41], [42]. Utilizing the above fact, the autocorrelation function $R_{Z\pm}(\tau)$ becomes [43, p.287]

$$R_{Z\pm}(\tau) = 4\pi^2 (N_+ + N_-)\delta(\tau) + 4\pi^2 (N_+ - N_-)^2. \tag{2.18}$$

The average number of positive clicks, $N_+$, is given by Rice:

$$N_+ = \int d\dot{\psi}\, p(\dot{\psi})\frac{\alpha}{4\pi} \left\{ \sqrt{1+(\frac{\dot{\psi}}{\alpha})^2}\ \mathrm{erfc}\left(\frac{r}{\sqrt{2}\,\sigma_n}\sqrt{1+(\frac{\dot{\psi}}{\alpha})^2}\right) \right.$$

$$\left. -\frac{\dot{\psi}}{\alpha}\, e^{-r^2/2\sigma_n^2}\ \mathrm{erfc}\left(\frac{r\dot{\psi}}{\sqrt{2}\,\sigma_n\alpha}\right) \right\} \quad . \tag{2.19}$$

where $p(\dot{\psi})$ is the probability density function of the modu-
lating signal $\dot{\psi}$, $\sigma_n^2$ is the average power of the input noise,
and erfc$(\cdot)$ is the complementary error function. Moreover,
$\alpha/2\pi$ is the r.m.s. bandwidth (or the effective bandwidth)
of the input noise and is defined as follows:

$$\frac{\alpha}{2\pi} = \frac{1}{2\pi} \sqrt{\frac{\sigma_{\dot{\xi}}^2}{\sigma_{\xi}^2}} \quad , \tag{2.20}$$

$$\sigma_{\xi}^2 = \int_0^\infty 2S_n(f)df \quad , \tag{2.21}$$

$$\sigma_{\dot{\xi}}^2 = (2\pi)^2 \int_0^\infty 2(f-f_o)^2 S_n(f)df ,$$

where $S_n(f)$ is the two-sided power spectral density of the
input noise. For the average number $N_-$ of the negative clicks,
the following relationship holds:

$$N_- = N_+ + \int d\dot{\psi}p(\dot{\psi})\frac{\dot{\psi}}{2\pi} e^{-r^2/2\sigma_n^2} \quad . \tag{2.22}$$

If the probability density function $p(\dot{\psi})$ of the modulating
signal is an even function with respect to zero value
(this is the model assumed in this analysis), the average
number of the positive clicks and that of the negative clicks
are equal.

The output power $N_{OZ\pm}$ due to the clicks is obtained by
utilizing the Fourier transformation of (2.18):

$$N_{OZ\pm} = \int_{-f_m}^{f_m} \left\{ \int_{-\infty}^\infty R_{Z\pm}(\tau)e^{-j2\pi f\tau}d\tau \right\} df = 16\pi^2 f_m N_+ \quad , \tag{2.23}$$

where $f_m$ is the cutoff frequency of the low-pass filter.

## 2.5.2 Random Noise Power

The Gaussian random noise power is derived by firstly obtaining the autocorrelation function $R_y(\tau)$ of $y$ in (2.10):

$$R_y(\tau)=R_\xi(\tau)\frac{1}{r^2} \ E[\cos(\psi(t+\tau)-\psi(t))] \ , \qquad (2.24)$$

where $R_\xi(\tau)$ is the autocorrelation function of $\xi$. For the Gaussian random process $\psi(t)$, the following relation is given by utilizing the characteristic function method [44]:

$$E[\cos(\psi(t+\tau)-\psi(t))]=\exp[-\{R_\psi(0)-R_\psi(\tau)\}]$$
$$\underset{=}{\Delta}R_L(\tau) \ , \qquad (2.25)$$

where $R_\psi(\tau)$ is the autocorrelation function of $\psi(t)$. The power spectral dendity $S_L(f)$ corresponding to $R_L(\tau)$, under the assumption that $R_\psi(0)\gg1$ (wideband FM), is [4, p.169]

$$S_L(f) \simeq \frac{1}{\sqrt{2\pi} \ \Delta f} \ \exp\{-\frac{f^2}{2(\Delta f)^2}\} \ . \qquad (2.26)$$

From the power spectral density $S_y(f)$ corresponding to $R_y(\tau)$, the power spectral density $S_{\dot{y}}(f)$ is obtained [43, p.351]:

$$S_{\dot{y}}(f)=4\pi^2f^2S_y(f) \ . \qquad (2.27)$$

Therefore, the random noise power $N_{O\dot{y}}$ becomes

$$N_{O\dot{y}}=\int_{-f_m}^{f_m} S_{\dot{y}}(f)df=\frac{1}{r^2} \ \frac{2\pi^2\sigma_n^2f_m^2\text{erf}(\sqrt{2})}{3\beta} \ . \qquad (2.28)$$

The derivation of (2.28) is described in Appendix B.

## 2.6 Output SNR

From expressions (2.15), (2.23), and (2.28), the output Signal-to-Noise power Ratio (SNR) is defined as

$$\left(\frac{S}{N}\right)_O = \frac{S_O}{N_{O\dot{y}} + N_{OZ\pm}} \quad . \tag{2.29}$$

## 2.7 Concluding Remarks

In this chapter, the detection system of the analog FM signal and its output SNR has been defined. The following chapter extends the analysis described in this chapter to the case where the input analog FM signal is subject to fading.

Chapter 3


ANALOG FREQUENCY MODULATION SYSTEM

IN FADING ENVIRONMENTS [45]-[47]


3.1  Introductory Remark

Since image information as a television signal is dete-
riorated more by the lower frequency component of the output
noise than the higher frequency component, a reasonable con--
sideration of the transmission method suitable to such a
information choose an analog FM system, which provides an
triangular noise spectrum at the detector output [48].
Therefore, the analog FM system is adopted for a broadcasting
satellite system, and the transmission experiment has been
already done [7].

The theoretical discussion on the output performance of
the analog FM system without a sufficient margin needs the
adoption of an analysis model which can deal with the phe-
nomenon around the so-called threshold region.  At and below
the threshold point, many impulsive clicks peculiar to analog
FM detection occur in addition to the continuous random
noise.  Although both of these noises degrade the detected
image, they have different effects to the eyesight, as
described in Ch. 1.  A viewing test [7], for instance, shows
that the clicks are perceptible when the number of clicks is
of the order of 1000 to 5000 per second.  To evaluate the
click noise quantitatively, this chapter adopts the Rice's
procedure which can deal with the random noise and the click
noise separately.

The improvement effects owing to the diversity tech-

niques combatting the effects of fading are also investigated
and three kinds of predetection diversity combining technique,
such as Selection Combining (SC), Equal-Gain Combining (EGC),
and Maximal-Ratio Combining (MRC) are compared from the view-
point of the improvement effects. In this case, the correla-
tion between two diversity branches which degrades the improve-
ment effect is also taken into consideration.

In this chapter, when analog FM is subject to nonselec-
tive $m$-distributed fading, the output noise characteristics,
the output SNR characteristics, and the improvement effects
by the predetection diversity techniques are described for a
system whose transmitter output power is limited as in the
case of satellite systems.


## 3.2 $m$-Distributed Fading

The $m$-distribution is a general model of the faded
envelope; it was formulated by Nakagami [22] in his study of
experimental data on high-frequency long distance propagation.
Its probability density function of envelope $r$, $p(r)$, is
given as

$$p(r) = \frac{2m^m r^{2m-1}}{\Gamma(m)\Omega^m} \exp\left(-\frac{mr^2}{\Omega}\right) \triangleq M(r,m,\Omega) , \qquad (3.1)$$

$$\Omega = E[r^2] = 2\sigma_c^2 ,$$

where $\sigma_c^2$ is the average carrier power and $\Gamma(\cdot)$ is the Gamma
function. The parameter $m$, which is called the fading figure,
is represented as

$$m = \frac{(E[r^2])^2}{E[(r^2 - E[r^2])^2]} \geq \frac{1}{2} , \qquad (3.2)$$

that is, $m$ is the inverse of the normalized variance of $r^2$.
By changing the value of $m$, various states of fading can be

represented: deep fading and shallow fading.  Especially,
the choice of $m=1$ corresponds to the Rayleigh fading, that
of $m=\frac{1}{2}$ to the one-sided Gaussian fading, and that of $m\rightarrow\infty$
to no fading.  In addition, by the appropriate selection of
the parameters $\Omega$ and $m$, the Nakagami-Rice distribution can
be approximately represented [49].  The plots of the m-
distribution are shown in Fig. 3.1 for typical values of $m$.
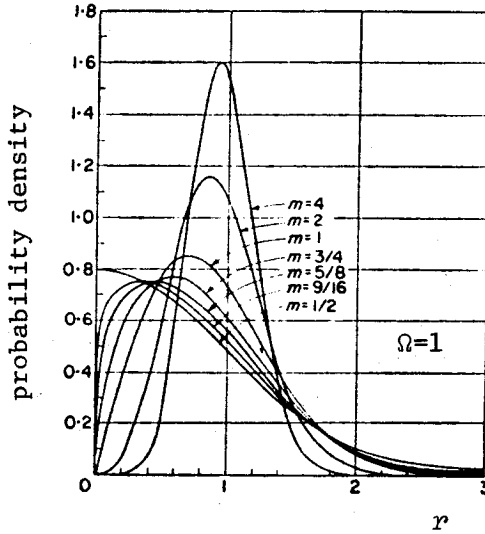
Fig. 3.1  $m$-Distribution.

## 3.3  Output SNR

The analysis described in Ch.2, which was applied to
the steady signal, now extends to the derivation of the out-
put SNR   in fading environments.  In the nonselective
$m$-distributed fading environments, the instantaneous envelope
follows the $m$-distribution and the phase follows the uniform
distribution; therefore, the envelope and the phase in (2.1)
are now time-varing: $r(t)$ and $\theta(t)$.  However, under the as-
sumption that the fading rate is sufficiently small compared
with the modulating  signal , the effects of time-variation
of the envelope and the phase may be neglected.  Hence, the

click or random noise power in the fading environments, can be obtained by averaging (2.23) or (2.28) over the random variables $r$ and $\theta$. In addition, the equations (2.23) and (2.28) are independent of $\theta$, so that only the averaging operation on $r$ is necessary. In this case, the average number of positive clicks, $[N_+]_F$, is

$$[N_+]_F = \int_0^\infty N_+ p(r) dr \; . \tag{3.3}$$

Upon substituting the equation (3.1) into the above equation and by utilizing formulas (A.1)-(A.5) found in Appendix A, the average number of clicks is calculated to be

$$[N_+]_F = \int d\dot{\psi}\, p(\dot{\psi}) \frac{\alpha}{4\pi} \left[ \sqrt{1+(\tfrac{\dot{\psi}}{\alpha})^2} - \frac{\frac{\dot{\psi}}{\alpha}}{(1+\frac{\rho_o}{m})^m} - \frac{\Gamma(m+\tfrac{1}{2})\{1+(\tfrac{\dot{\psi}}{\alpha})^2\}}{\Gamma(m)} \right.$$

$$\cdot \left(\frac{4\rho_o}{m\pi}\right)^{\frac{1}{2}} \left\{1 + \frac{\rho_o(1+(\tfrac{\dot{\psi}}{\alpha})^2)}{m}\right\}^{-(m+\frac{1}{2})} {}_2F_1\left(1, m+\tfrac{1}{2}; \tfrac{3}{2}; \frac{1}{1+\frac{m}{(1+(\tfrac{\dot{\psi}}{\alpha})^2)\rho_o}}\right)$$

$$+ \frac{(\tfrac{\dot{\psi}}{\alpha})^2 \Gamma(m+\tfrac{1}{2})}{\Gamma(m)} \left(\frac{4\rho_o}{m\pi}\right)^{\frac{1}{2}} \left\{1 + \frac{(1+(\tfrac{\dot{\psi}}{\alpha})^2)\rho_o}{m}\right\}^{-(m+\frac{1}{2})}$$

$$\cdot {}_2F_1\left(1, m+\tfrac{1}{2}; \tfrac{3}{2}; \frac{(\tfrac{\dot{\psi}}{\alpha})^2 \rho_o}{m+(1+(\tfrac{\dot{\psi}}{\alpha})^2)\rho_o}\right) \Big] \triangleq N_+(m, \rho_o) \; , \tag{3.4}$$

$$\left( \rho_o = \frac{\sigma_c^2}{\sigma_n^2} \right)$$

where $\rho_0$ is the average Carrier-to-Noise power Ratio (CNR) and $_2F_1(\cdot,\cdot;\cdot;\cdot)$ is the generalized hypergeometric function. The click noise power $[N_{OZ\pm}]_F$ is

$$[N_{OZ\pm}]_F = 16\pi^2 f_m [N_+]_F \ . \tag{3.5}$$

The Gaussian random noise power $[N_{O\dot{y}}]_F$ is obtained in a similar manner:

$$[N_{O\dot{y}}]_F = [\frac{1}{r^2}]_F \ \frac{2\pi^2 \sigma_n^2 f_m^2 \mathrm{erf}(\sqrt{2})}{3\beta} \ , \tag{3.6}$$

where

$$[\frac{1}{r^2}]_F = \int_0^\infty \frac{1}{r^2} p(r) dr \ . \tag{3.7}$$

In the case of the $m$-distributed fading, the above equation is calculated as

$$[\frac{1}{r^2}]_F = \frac{m\Gamma(m-1)}{\Gamma(m)\Omega} \triangleq G(m,\Omega) \ , \quad m>1 \ . \tag{3.8}$$

From (2.15),(3.5) , and(3.6), the output SNR $\left(\frac{S}{N}\right)_F$ in the $m$-distributed fading environments is determined as

$$\left(\frac{S}{N}\right)_F = \frac{S_0}{[N_{OZ\pm}]_F + [N_{O\dot{y}}]_F} \ . \tag{3.9}$$

## 3.4  Improvement by Predetection Diversity Techniques

In this section, three types of predetection diversity technique  are considered: Selection Combining (SC), Equal-Gain Combining (EGC), and Maximal-Ratio Combining (MRC). The number of diversity branches is assumed to be two from the practical point and the block diagram is shown in Fig. 3.2.
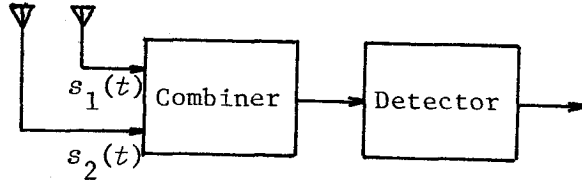
Fig. 3.2 Predetection Diversity System.

In discussing the improvement effects owing to the diversity
techniques, consideration of the correlation between the two
branches is of great importance since such correlation will
deteriorate the output SNR performance. It is thus assumed
that the two branches are correlated with the power correla-
tion coefficient of $k^2$;

$$k^2 = \frac{E[(r_1^2-\Omega)(r_2^2-\Omega)]}{\sqrt{E[(r_1^2-\Omega)^2]E[(r_2^2-\Omega)^2]}} .$$  (3.10)

It is also assumed that the input signals on two deversity
branches are subject to nonselective $m$-distributed fading
and have equal average power, and that the input noise
components on the two diversity branches are uncorrelated
Gaussian random processes of equal variance.

The means of deriving the probability density functions
of the combined signals is described in detail by Brennan [27].
Assuming $m$-distributed fading, the probability density func-
tions are given as follows [50]:

(1) Selection Combining (SC)

$$p_S(r) = \int_0^1 dx \int_0^\pi d\zeta \; c_S \; w_S^{2m} \; M(r, 2m, 2\Omega\sqrt{1-k^2} \; w_S), \quad (3.11)$$

$$c_S = [2^{2m}(2m-1)/\pi]x^{2m-1} \sin^{2m-2}\zeta,$$

$$w_S = \sqrt{1-k^2}/\{1+x^2-2x\sqrt{k^2} \cos\zeta\}.$$

(2) Equal-Gain Combining (EGC)

$$p_E(r) = \int_0^1 dx \int_0^\pi d\zeta \; c_E \; w_E^{2m} \; M(r, 2m, 2\Omega\sqrt{1-k^2} \; w_E), \quad (3.12)$$

$$c_E = [2(2m-1)/\pi][1-(1-x)^2]^{2m-1} \sin^{2m-2}\zeta,$$

$$w_E = \sqrt{1-k^2}/[\{1+(1-x)^2\}-\{1-(1-x)^2\}\sqrt{k^2} \cos\zeta].$$

(3) Maximal-Ratio Combining (MRC)

$$p_M(r) = \int_0^\pi d\zeta \; c_M \; w_M^{2m} \; M(r, 2m, 2\Omega\sqrt{1-k^2} \; w_M), \quad (3.13)$$

$$c_M = \Gamma(m+\tfrac{1}{2}) \sin^{2m-1}\zeta/\{\sqrt{\pi}\Gamma(m)\},$$

$$w_M = \sqrt{1-k^2}/[1-\sqrt{k^2}\cos\zeta].$$

The click and random noise power owing to the diversity techniques can be obtained in a similar manner as described in Sec. 3.3. The click noise power $[N_{OZ\pm}]_*$ is

$$[N_{OZ\pm}]_* = 16\pi^2 f_m [N_+]_*, \quad (3.14)$$

$$[N_+]_* = \int_0^1 dx \int_0^\pi d\zeta \; c_* \; w_*^{2m} \; N_+(2m, 2\rho_\circ\sqrt{1-k^2} \; w_*), \quad (3.15)$$

- 21 -

where the symbol " * " denotes the type of the diversity technique: the replacement of " * " with " $S$ " corresponds to SC, with " $E$ " to EGC, and with " $M$ " to MRC. The Gaussian random noise power $[N_{Oy}^{\bullet}]_*$ is

$$[N_{Oy}^{\bullet}]_*=[\frac{1}{r^2}]_*\ \frac{2\pi^2\sigma_n^2 f_m^2\mathrm{erf}(\sqrt{2})}{3\beta}\ , \qquad (3.16)$$

$$[\frac{1}{r^2}]_*= \int_0^1 dx \int_0^\pi d\zeta\ c_*\ w_*^{2m}G(2m, 2\Omega\sqrt{1-k^2}\ w_*)\ . \qquad (3.17)$$

The output SNR is finally obtained as

$$(\frac{S}{N})_*=\frac{S_O}{[N_{OZ\pm}]_*+[N_{Oy}^{\bullet}]_*}\ . \qquad (3.18)$$

## 3.5  System Comparison

The numerical calculations of (3.4),(3.9),(3.14)-(3.18) exemplify the following results:

  (1) Relations of the average number of clicks to the fading figures and to the input CNRs (refer to Figs. 3.3-3.6).

  1) As $\rho_o$ and/or $m$ increases (fading becomes shallower for greater $m$), the average number decreases.

  2) When the input signals are uncorrelated ($k=0$), MRC has the smallest average number, EGC has the second smallest, and SC has the largest. When they are correlated, the smaller the correlation coefficient , the better the performance.

  3) By the utilization of these graphs, it is possible to obtain the average number of dots $N$ observed on the picture. If the input BPF bandwidth is defined to be $2B$, then

$$N=2N_+=2 \cdot \frac{\alpha}{4\pi} \cdot \text{(the value on the graph)}$$

$$= \frac{2B}{\sqrt{12}} \cdot \text{(the value on the graph)} .$$

For example, in the case of no diversity, $N$ is calcu-
lated to be about 6400 for $m=10$, $\rho_0=10$dB, and $2B=25$MHz.
Conversely, assuming that the number of 5000 per second
(corresponding to the value of $6.9 \times 10^{-4}$ on the graph)
is the maximum perceptible value, the required CNRs
under the condition of $m=2$ and $k=0$ can be obtained
from Figs. 3.5 and 3.6: 18.1dB for no diversity,
11.6dB for SC, 10.1dB for EGC, and 9.7dB for MRC.

(2) Relations between the power ratios of click noise to
   random noise and fading figures (refer to Figs. 3.7
   and 3.8).

  1) In the case of no diversity, the increase of the power
     ratio by the decrease of $m$ implies that the click
     noise is more strongly affected than the random noise
     by fading.

  2) The result that the employment of the diversity tech-
     niques decreases the power ratio compared with the
     case of the no diversity, implies that diversity offers
     greater improvement effects to the click noise than
     to the random noise.  In addition, since MRC has the
     largest improvement effects, the threshold phenomenon
     caused by the click noise occurs at the lowest CNR for
     fixed $m$ as in Figs. 3.9 and 3.10.

  3) The reason  why fading affects the click noise more
     strongly than the random noise, can be explained as
     follows : Since the inphase noise component with
     respect to the input signal contributes to the occur-

rence of clicks, the fluctuation of the signal
envelope increase the chance of its occurrence. That
the employment of the diversity techniques decreases
the click noise power can be also explained in a
similar manner, because its employment decreases the
percentage of falling into the lower signal envelope
level.

(3) Relations between the output SNRs and the input CNRs
(refer to Figs. 3.9 and 3.10).

1) The output SNR performance becomes better as $m$
increases, and MRC has the best performance when the
diversity techniques are utilized. Especially, the
difference between the performance for MRC and that
for EGC is small, and its difference tends to become
smaller as $m$ increases.

2) In the case of $m=2$, the assumption that the output
SNR of 40dB is necessary to detect the image informa-
tion, requires the input CNR of 21.5dB for no diver-
sity, 11.5dB for MRC with $k=0$, 12dB for MRC with $k=0.6$,
and 14.5dB for MRC with $k=0.9$. Therefore, it is shown
that considerable diversity improvement effects can
be obtained even in the case of high correlation.

3) The result for $m=100$ is also illustrated in Fig. 3.10,
and this result is consistent with that analyzed for
the no fading condition. Therefore, the analysis
described in this chapter can be generalized to in-
clude the case of no fading.
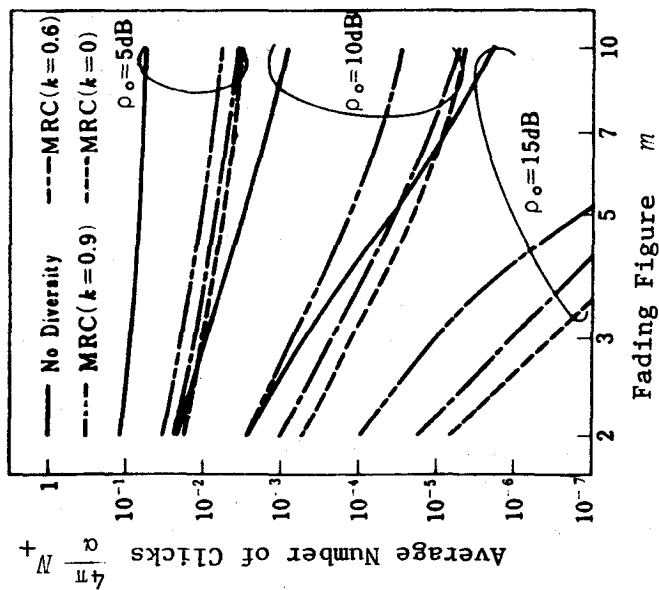
Fig. 3.4 Average Number of Clicks vs. Fading Figures.
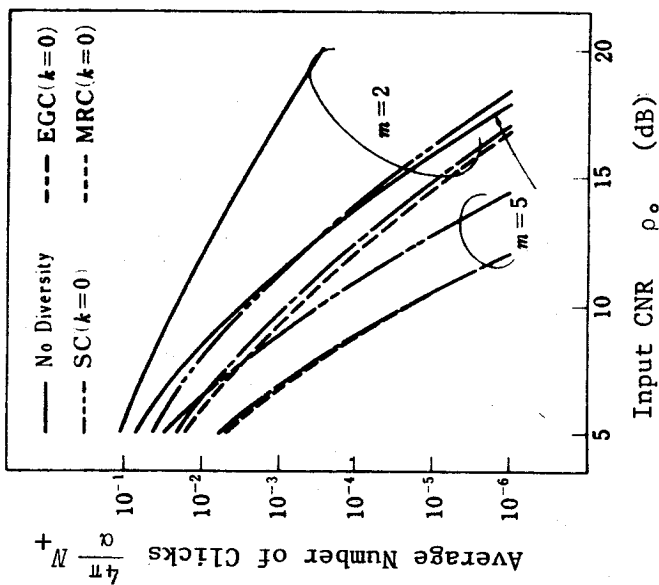


Fig. 3.3 Average Number of Clicks vs. Fading Figures.

Fig. 3.6   Average Number of Clicks
vs. Input CNRs.



Fig. 3.5   Average Number of Clicks
vs. Input CNRs.

No Diversity —  EGC(k=0)

SC(k=0) —·— MRC(k=0)

$\rho_o = 5dB$

$\rho_o = 10dB$

$\rho_o = 15dB$

$10^2$

$10$

$1$

$10^{-1}$

$10^{-2}$

Power Ratio $\dfrac{[N_{OZ^{\pm}}]_*}{[N_{O_y}]_*}$

2    3    5    7    10

Fading Figure    $m$

Fig. 3.7   Power Ratios of Click Noise
to Random Noise vs. Fading
Figures.

No Diversity —--— MRC(k=0.6)

MRC(k=0.9) —·— MRC(k=0)

$\rho_o = 5dB$

$\rho_o = 10dB$

$\rho_o = 15dB$

$10^2$

$10$

$1$

$10^{-1}$

$10^{-2}$

Power Ratio $\dfrac{[N_{OZ^{\pm}}]_*}{[N_{O_y}]_*}$

2    3    5    7    10
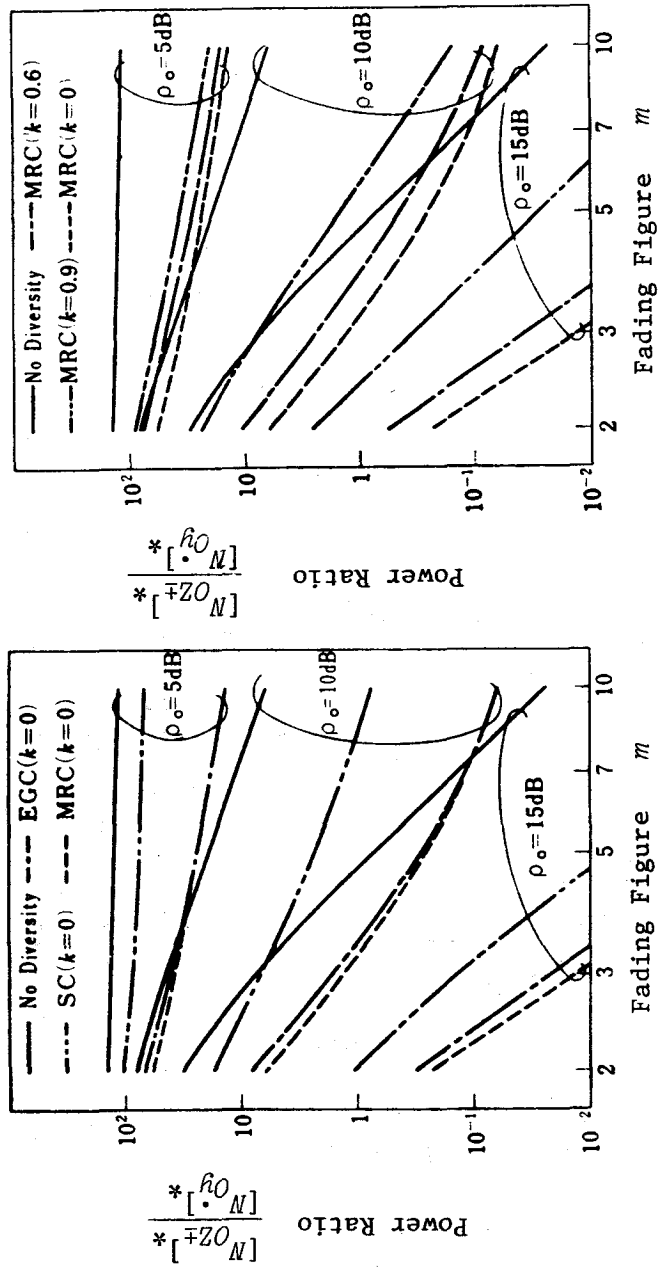
Fading Figure    $m$

Fig.  3.8   Power Ratios of Click Noise
to Random Noise vs. Fading
Figures.

- 27 -
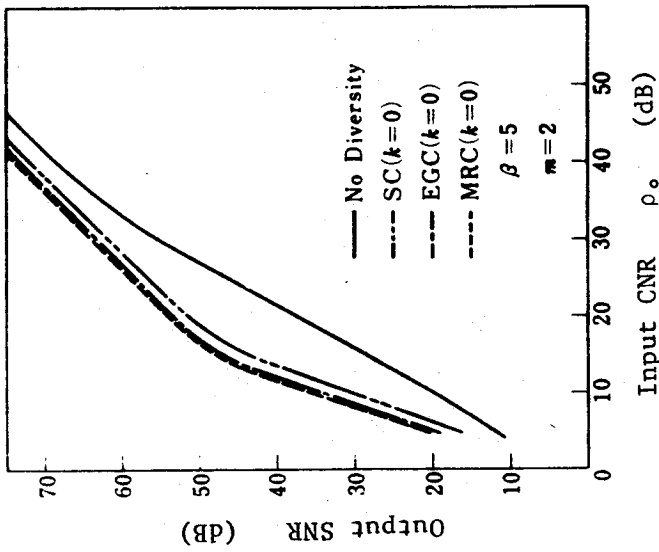
Fig. 3.9 Output SNRs vs. Input CNRs.
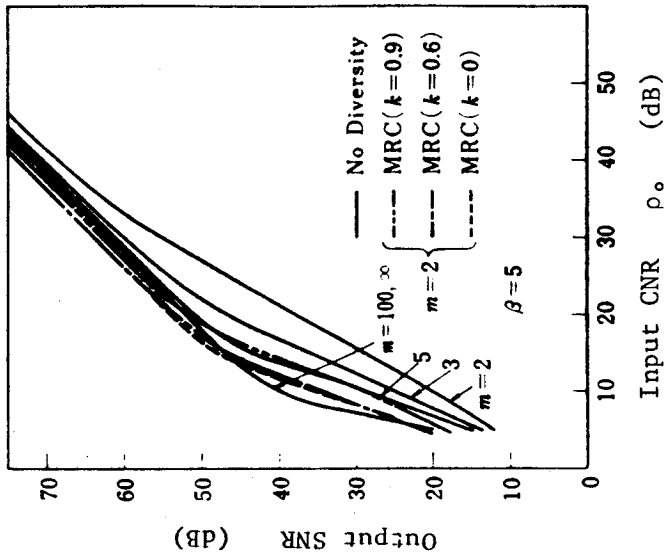
Fig. 3.10 Output SNRs vs. Input CNRs.

## 3.6 Concluding Remarks

In this chapter, the output noise and output SNR characteristics of the analog FM system in the nonselective $m$-distributed fading environments have been described including the improvement effects owing to the predetection diversity techniques.

The main results are summarized as follows:

(1) Fading affects the click noise more strongly than the random noise.

(2) Much more diversity improvement effects can be obtained for the click noise than for the random noise.

(3) Better output SNR performance can be obtained with smaller correlation between two diversity branches.

(4) MRC is the most efficient diversity technique.

(5) The analysis described in this chapter is also applicable to the case of no fading.

Chapter 4


## DIGITAL FREQUENCY MODULATION SYSTEM


### 4.1 Introductory Remark

This chapter describes the error rate performance of
the digital FM signal when detected by a conventional limiter-
discriminator with an integrate-and-dump filter. The error
rate can be obtained by, 1) deriving the probability density
function of the detector output, which consists of the
desired signal, random noise, and click noise, and then
2) integrating this probability density function over the
error region.

### 4.2 Analysis Model

The system under consideration is a binary digital FM
(FSK[†]: Frequency Shift Keying) system employing a conventional
limiter-discriminator with a postdetection filter [51]-[52].
As shown in Fig. 4.1, the received FSK signal is corrupted
by white Gaussian noise, passed through a band-pass filter
at the carrier frequency $f_0$ with bandwidth $2B$, detected by
the frequency-discriminator followed by an integrate-and-
dump filter, and then subsequently sampled.

---

† In this thesis, the term " FSK " is used to mean " digital
 FM " for the sake of expressional simplicity.
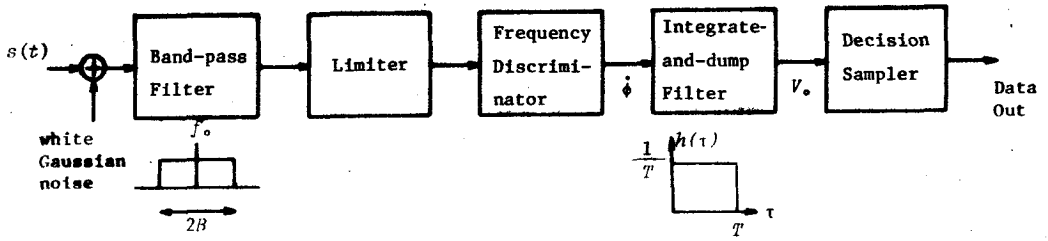
Fig. 4.1   Detection System for Digital
Frequency Modulation Signal.

The input FSK signal $s(t)$ can be expressed by defining $\psi(t)$ in (2.1) as follows:

$$s(t) = r\cos[\omega_0 t + \psi(t) + \theta] \ , \tag{4.1}$$

$$\left\{ \begin{aligned} &\psi(t) = \Delta\omega_d \int_{-\infty}^{t} f(t')dt' \\[2em] &f(t) = \sum_{i=-\infty}^{\infty} 2(a_i - \frac{1}{2}) \ g(t-iT) \\[1em] &\quad a_i = \begin{cases} 1, & \text{"mark"} \\ 0, & \text{"space"} \end{cases} \\[1em] &\quad g(t) = \begin{cases} 1, & 0 \le t \le T \\ 0, & \text{otherwise} \end{cases} \\[1em] &\quad T \quad : \quad \text{digit duration} \\ &\quad \Delta\omega_d : \quad \text{peak angular frequency deviation} \ . \end{aligned} \right.$$

The approximate  composite phase $\phi$ corresponding to (2.8) is given in the alternative form:

- 31 -

$$\phi \simeq \psi + \theta + a \; \frac{\cos\theta}{r} - b \; \frac{\sin\theta}{r} \; , \qquad\qquad (4.2)$$

$$a \triangleq \eta\cos\psi - \xi\sin\psi, \quad b \triangleq \xi\cos\psi + \eta\sin\psi \; .$$

Therefore, the output of the discriminator becomes

$$\dot\phi \simeq \dot\psi + \dot{a} \; \frac{\cos\theta}{r} - \dot{b} \; \frac{\sin\theta}{r} + 2\pi(Z_+ - Z_-) \; , \qquad (4.3)$$

where $2\pi(Z_+ - Z_-)$ is the additional term on account of the positive and negative clicks as in (2.9). In the above equation, let $\dot{u}$ be defined as

$$\dot{u} = \dot{a} \; \frac{\cos\theta}{r} - \dot{b} \; \frac{\sin\theta}{r} \; , \qquad\qquad (4.4)$$

then $\dot{u}$ is Gaussian distributed and its probability density function $p(\dot{u})$ is represented by

$$p(\dot{u}) = \frac{1}{\sqrt{2\pi} \; M} \; \exp\left( - \frac{\dot{u}^2}{2M^2} \right), \qquad\qquad (4.5)$$

$$M^2 = E[\dot{u}^2] = \frac{E[\dot{a}^2]}{r^2} \; .$$

## 4.3 Probability Density Function of Detector Output

The derivation of the error rate necessitates the probability density function of the integrate-and-dump filter output.

The impulse response of the integrate-and-dump filter $h(\tau)$ is defined as

$$h(\tau) = \begin{cases} \dfrac{1}{T} \; , & 0 \le \tau \le T \\[2ex] 0 \; , & \text{otherwise} \; . \end{cases} \qquad\qquad (4.6)$$

- 32 -

Sampled at the end of the digit $t_s[=(n+1)T: n=\cdots,-1,0,1,\cdots]$, the sampled output of the integrate-and-dump filter $V_o$ becomes

$$V_o \triangleq \dot{\psi}_o + \dot{u}_o + Z_o \ , \qquad (4.7)$$

where $\dot{\psi}_o$ is a component due to the signal, $\dot{u}_o$ to the random Gaussian noise, and $Z_o$ to the click noise. Here the signal component $\dot{\psi}_o$ is given as follows:

$$\dot{\psi}_o = \begin{cases} +\Delta\omega_d \ , & \text{"mark"} \\ -\Delta\omega_d \ , & \text{"space"} \ . \end{cases} \qquad (4.8)$$

The random noise component $\dot{u}_o$ is represented by

$$\dot{u}_o = \dot{a}_o \frac{\cos\theta}{r} - \dot{b}_o \frac{\sin\theta}{r} \ , \qquad (4.9)$$

$$\dot{a}_o = [\dot{a} \otimes h]_{t=t_s} \ , \quad \dot{b}_o = [\dot{b} \otimes h]_{t=t_s} \ ,$$

where " $\otimes$ " denotes the time convolution.

If the input random process to the linear filter is Gaussian distributed, the output random process is also Gaussian distributed [44, p.189]. Therefore, the probability density function $p(\dot{v}_o \triangleq \dot{\psi}_o + \dot{u}_o \mid \dot{\psi}_o = \pm\Delta\omega_d)$ has the form

$$p(\dot{v}_o \mid \dot{\psi}_o = \pm\Delta\omega_d) = \frac{1}{\sqrt{2\pi}\,M_o} \exp\left(- \frac{(\dot{v}_o \mp \Delta\omega_d)^2}{2M_o^2}\right) \ , \qquad (4.10)$$

$$M_o^2 = E[\dot{u}_o^2] = \frac{E[\dot{a}_o^2]}{r^2} = \frac{2\sigma_n^2 f_o(\beta)}{r^2 T^2} \ ,$$

$$f_o(\beta) = 1 - \frac{\sin\pi(\beta+1)}{\pi(\beta+1)} \ ,$$

where $M_o^2$ is the average power of the random noise component at the sampling instants and is given in Appendix C. The click noise component $Z_o$ is

$$Z_o = \frac{2\pi}{T} \int\limits_{nT}^{(n+1)T} \{ \sum_{k=-\infty}^{\infty} \delta(t-t_k) - \sum_{l=-\infty}^{\infty} \delta(t-t_l) \} dt \ . \qquad (4.11)$$

As described in Ch. 2, it is assumed that the clicks are independent of one another and follow the Poisson process. Therefore, $Z_o$ is the difference of two independent Poisson processes and its probability density function $p(Z_o)$ is given as [53]:

$$p(Z_o) = \sum_{\mu=-\infty}^{\infty} \exp[-(\lambda_+ + \lambda_-)] \left(\frac{\lambda_+}{\lambda_-}\right)^{\frac{\mu}{2}} I_{|\mu|} (2\sqrt{\lambda_+\lambda_-}) \delta(Z_o - \frac{2\pi\mu}{T}) \ , \quad (4.12)$$

where

$\lambda_+$, $\lambda_-$: the average number of positive and negative clicks during $T$ sec.[†],

$$\begin{cases} \lambda_+ = N_+ T \\ \lambda_- = N_- T \end{cases}$$

$\mu$: the remainder after taking the number of negative clicks from that of the positive clicks,

$I_{|\mu|}$: the modified Bessel function of integer order $|\mu|$.

The convolution of (4.10) and (4.12) establishes the probability density function of $V_o$ $p(V_o)$ as:

---

[†] For the mark signal, the average number per second can be obtained in (2.19) and (2.22) by setting $p(\dot{\psi}) = \delta(\dot{\psi} - \Delta\omega_d)$.

$$p(V_\circ|\dot{\psi}_\circ=\pm\Delta\omega_d)=\sum_{\mu=-\infty}^{\infty}\exp[-(\lambda_++\lambda_-)]\left(\frac{\lambda_+}{\lambda_-}\right)^{\frac{\mu}{2}}I_{|\mu|}(2\sqrt{\lambda_+\lambda_-})$$

$$\cdot\frac{1}{\sqrt{2\pi}\,M_\circ}\exp\left\{-\frac{(V_\circ\mp\Delta\omega_d-2\pi\mu/T)^2}{2M_\circ^2}\right\}.\qquad(4.13)$$

## 4.4  Error Rate

The integration of the probability density function given in (4.13) over the error region derives the error rate of the FSK signal.  On the assumption that the mark and space signals are equally likely to occur, the detector decides that $\dot{\psi}_\circ=\Delta\omega_d$ if $V_\circ>0$ and that $\dot{\psi}_\circ=-\Delta\omega_d$ if $V_\circ<0$ [54, Ch.3]. In addition, the error rate for the mark signal and that for the space signal become equal, because $\lambda_-$ observed in a positive digit interval is equal to $\lambda_+$ observed in a negative digit interval.  Therefore, the error rate $P_N$ is given as

$$P_N=\int_{-\infty}^{0}p(V_\circ|\dot{\psi}_\circ=\Delta\omega_d)dV_\circ$$

$$=\int_{0}^{\infty}p(V_\circ|\dot{\psi}_\circ=-\Delta\omega_d)dV_\circ.\qquad(4.14)$$

Substituting (4.13) into (4.14) yields

$$P_N=\frac{1}{2}\sum_{\mu=-\infty}^{\infty}\exp[-(\lambda_++\lambda_-)]\left(\frac{\lambda_+}{\lambda_-}\right)^{\frac{\mu}{2}}I_{|\mu|}(2\sqrt{\lambda_+\lambda_-})$$

$$\cdot\mathrm{erfc}\left([\Delta\omega_d+2\pi\mu/T]/\sqrt{2}M_\circ\right).\qquad(4.15)$$

Since the above equation is mathematically complex, it is not easy to extend the analysis to the next stage to be described in the following chapter. Thus, the simplification of (4.15) is attempted in the following.

In general, with existence of modulating signals, the average numbers $N_+$ and $N_-$ become unequal. The fact that for the mark signal the majority of clicks occur in the negative directions [6, p335] makes it reasonable to neglect the positive clicks:

$$N_+ << N_- \quad \text{or} \quad \lambda_+ << \lambda_- \quad . \tag{4.16}$$

Upon utilizing (2.22) and the above fact, $N_-$ and $\lambda_-$ are reduced to

$$N_- \simeq \frac{\Delta\omega_d}{2\pi} e^{-r^2/2\sigma_n^2} , \tag{4.17}$$

$$\lambda_- \simeq \frac{\beta}{2} e^{-\rho} ,$$

where $\beta (=\Delta\omega_d T/\pi)$ is the modulation index and $\rho (=r^2/2\sigma_n^2)$ is the input CNR. In addition, under the condition of the comparatively high input CNR, the probability that many clicks occur during one digit duration $T$ is very small, $i.e.,$ $\lambda_+$ and $\lambda_- << 1$, and at most only one click occurs during $T$. Therefore, the following approximate expressions can be utilized:

$$I_{|\mu|}(2\sqrt{\lambda_+\lambda_-}) \simeq (\lambda_+\lambda_-)^{\frac{|\mu|}{2}} \frac{1}{|\mu|!} , \tag{4.18}$$

$$\exp[-(\lambda_++\lambda_-)] \simeq 1 \quad .$$

Substitution of (4.17) and (4.18) into (4.15), and the choice of μ=0 and 1 in (4.15), yield the final expression for the error rate as follows:

$$P_N = \frac{1}{2}\,\mathrm{erfc}\,\Big(\frac{\pi\beta\sqrt{\rho}}{\sqrt{2}f_o(\beta)}\Big) + \frac{\beta}{4}\,e^{-\rho}\,\mathrm{erfc}\,\Big(\frac{\pi(\beta-2)\sqrt{\rho}}{\sqrt{2}f_o(\beta)}\Big) \triangleq P_N(r)\ .\quad (4.19)$$

## 4.5 Concluding remarks

In this chapter, the detection system of the FSK signal and its error rate have been discussed. The following chapter extends the analysis described in this chapter to the case where the input FSK signal is subject to fading.

Chapter 5

# DIGITAL FREQUENCY MODULATION SYSTEM

# IN FADING ENVIRONMENTS  [55]-[57]


## 5.1  Introductory Remark

Although many authors have investigated the error rate
performance of FSK systems in fading environments, their
fading models have been assumed to be either the Rayleigh[58] or
Rician distribution.  Furthermore, the employed diversity
techniques have been assumed to be the three kinds of pre-
detection type such as SC, EGC, and MRC without the consider-
ation  of the correlation between two diversity branches.

In this chapter, under the assumption that the FSK signal
is subject to nonselective $m$-distributed fading as described
in Ch. 3, its error rate is derived by the extension of the
analysis described in Ch. 4.  Furthermore, two other diversity
techniques in addition to the three kinds of predetection type
described in Ch. 3 are considered: Switch-and-Stay diversity
[59] included in predetection diversity, and postdetection
diversity [60]-[61] which has the advantage of simple imple-
mentation since the knowledge on the status of the fading channel
is not necessary.  In discussing the improvement effects owing
to the diversity techniques, the effect of the correlation
between two diversity branches are also taken into account.

In the case of the Switch-and-Stay diversity, a design
method of an optimum switching level which attains a minimum
error rate is shown.


## 5.2 Error Rate

Under the assumption that the input FSK signal is subject

to the nonselective $m$-distributed fading (as described in Sec. 3.2), the envelope may be regarded as constant during one digit duration $T$. Therefore, averaging the result given in Ch. 4 over the random variable $r$ yields the error rate of the FSK signal in the environments of interest, $P_F$, as

$$P_F = \int_0^\infty P_N(r)p(r)dr$$

$$= \frac{1}{2} - \frac{\Gamma(m+\frac{1}{2})}{\sqrt{\pi}\Gamma(m)} \left\{ \frac{\pi\beta\sqrt{\rho_0}}{\sqrt{2mf_0(\beta)}} \right\} \left\{ 1 + \frac{\pi^2\beta^2\rho_0}{2mf_0(\beta)} \right\}^{-(m+\frac{1}{2})}$$

$$\cdot {}_2F_1 \left( 1, m+\frac{1}{2}; \frac{3}{2}; \frac{\frac{\pi^2\beta^2\rho_0}{2mf_0(\beta)}}{1+\frac{\pi^2\beta^2\rho_0}{2mf_0(\beta)}} \right) + \frac{\beta}{4} \left( \frac{m}{m+\rho_0} \right)^m$$

$$\cdot \left\{ 1 - \frac{2\Gamma(m+\frac{1}{2})}{\sqrt{\pi}\Gamma(m)} \left( \frac{\pi(\beta-2)\sqrt{\rho_0}}{\sqrt{2(m+\rho_0)f_0(\beta)}} \right) \left( 1 + \frac{\pi^2(\beta-2)^2\rho_0}{2(m+\rho_0)f_0(\beta)} \right)^{-(m+\frac{1}{2})} \right.$$

$$\left. \cdot {}_2F_1 \left( 1, m+\frac{1}{2}; \frac{3}{2}; \frac{\frac{\pi^2(\beta-2)^2\rho_0}{2(m+\rho_0)f_0(\beta)}}{1+\frac{\pi^2(\beta-2)^2\rho_0}{2(m+\rho_0)f_0(\beta)}} \right) \right\} \triangleq P_F(m,\rho_0) ,\qquad (5.1)$$

by the utilization of (3.1), (4.19) and the formulas (A.1)– (A.5) in Appendix A.


## 5.3  Improvement by Diversity Techniques

The diversity techniques are classified into two kinds, depending on the place at which the combiner is located: the predetection diversity was described in Ch. 3 and the postdetection diversity is shown in Fig. 5.1.

It has been assumed that the number of diversity branches is two (from the practical point of view) and that the input noise components on the two branches are Gaussian distributed and mutually independent. Additionally, in the following analysis, the correlation between two branches is considered, except for the Switch-and-Stay diversity.
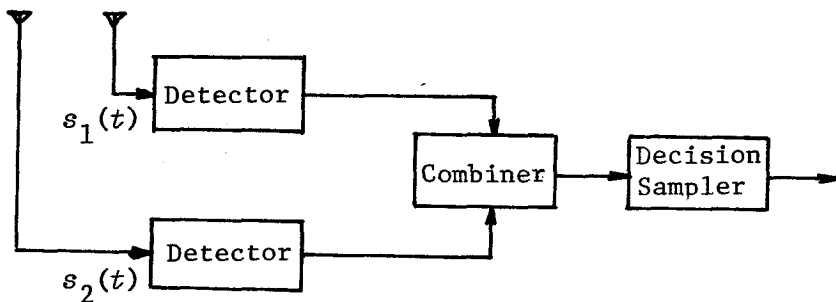
Fig. 5.1  Postdetection Diversity System.

### 5.3.1  Predetection Diversity

Four kinds of predetection diversity technique  are con-
sidered: Switching[†], Selection combining, Equal-Gain Combining,
and Maximal-Ratio Combining diversity technique.  The predetec-
tion diversity techniques, except for the Switching diversity,
have been previously described in Ch. 3 and the error rates
can be expressed similarly.  By the utilization of (5.1), the
error rates, $P_S$ for the Selection Combining, $P_E$ for the Equal-
Gain Combining, $P_M$ for the Maximal − Ratio Combining, are given
as follows:

$$P_* = \int_0^1 dx \int_0^\pi d\zeta \ c_* \ w_*^{2m} \ P_F(2m, 2\rho_o \sqrt{1-k^2} \ w_*) \ , \qquad (5.2)$$

where the symbol "$*$" is the same as indicated in Sec. 3.4,
and $c_*$ and $w_*$ are given in (3.11)-(3.13).

---

[†] Switching diversity is equivalent to Scanninig diversity
named by Brennan,

There are two kinds of Switching diversity technique:
Switch-and-Stay diversity and Switch-and-Examine diversity.
In this thesis, however, the analysis is confined to the former,
whose strategy is described as follows: the instantaneous en-
velope of the input signal is monitored; if it falls below a
predetermined switching level, the antenna switching is acti-
vated, thus selecting the other branch.  In such a case, even
if the second branch is also in a fade, the antenna switching
is not activated.  In the case of the Switch-and-Stay diversity
technique (SS), the combiner circuit in Fig. 5.1 is replaced
by a switching circuit comforming to the above strategy.

When the two branches are uncorrelated, the probability
density function for the output of the switching circuit, $P_{SS}(r)$,
is given by Rustako [59]:

$$p_{SS}(r) = \begin{cases} (1+c)p(r) , & r \geq A_S \\ c\, p(r) , & r \leq A_S , \end{cases} \tag{5.3}$$

where $A_S$ is the switching level and $c$ is determined as

$$c = \int_0^{A_S} p(r)dr . \tag{5.4}$$

The error rate $P_{SS}$ for $SS$ is given by the utilization of (4.19):

$$\begin{aligned} P_{SS} &= \int_0^\infty P_N(r)p_{SS}(r)dr \\ &= \int_0^{A_S} c\, P_N(r)p(r)dr + \int_{A_S}^\infty (1+c)P_N(r)p(r)dr \\ &= (1+c)\int_0^\infty P_N(r)p(r)dr - \int_0^{A_S} P_N(r)p(r)dr . \end{aligned} \tag{5.5}$$

- 41 -

Therefore, the substitution of (3.1) into the above equation yields the error rate in the $m$-distributed fading environments:

$$P_{SS} = (1+c)P_F(m,\rho_o) - \frac{m^m H^m}{\Gamma(m)} \int_0^1 \left\{ \mathrm{erfc}\left(\frac{\pi\beta\sqrt{\rho_o H}\ x}{\sqrt{2}f_o(\beta)}\right) \right.$$

$$\left. + \frac{\beta}{2}\ e^{-\rho_o Hx^2}\ \mathrm{erfc}\left(\frac{\pi(\beta-2)\sqrt{\rho_o H}x}{\sqrt{2}f_o(\beta)}\right) \right\} x^{2m-1} e^{-mHx^2} dx\ , \quad (5.6)$$

$$\begin{cases} H = \dfrac{A_S^2}{\Omega} \\[2mm] c = \dfrac{1}{\Gamma(m)}\ \gamma(m,mH) \end{cases}$$

where $\gamma(\cdot,\cdot)$ is the incomplete Gamma function and $P_F(m,\rho_o)$ is given in (5.1).

The selection of the value of $A_S$ is a very important factor on the error rate performance. As is easily known from (5.5), when $A_S$ is zero or infinity, $P_{SS}$ reduces to $P_F$. The optimum switching level $A_{SOP}$, which attains the minimum error rate, can be obtained from the differentiation of (5.5) with respect to $A_S$:

$$\frac{\partial P_{SS}}{\partial A_S} = \frac{\partial c}{\partial A_S} \int_0^\infty P_N(r)p(r)dr - \frac{\partial}{\partial A_S} \int_0^{A_S} P_N(r)p(r)dr$$

$$= p(A_S) \int_0^\infty P_N(r)p(r)dr - p(A_S)P_N(A_S)$$

$$= p(A_S)[P_F - P_N(A_S)]\ . \qquad (5.7)$$

Consequently, the level $A_{SOP}$ proves to be the solution to the following equation:

$$P_N(A_S) = P_F \quad . \tag{5.8}$$

This equation shows that the optimum switching level $A_{SOP}$ is the envelope for the no fading condition which gives the error rate equal to that for the fading condition. To verify the above description graphically, the relation between $P_{SS}$ and $A_S^2/A_{SOP}^2$ is shown in Fig. 5.2, where $P_{SSO}$ is the error rate in the case of the optimum switching level. These curves clarify that the shallower the fading, the more the degradation due to the offset from the optimum level appears.
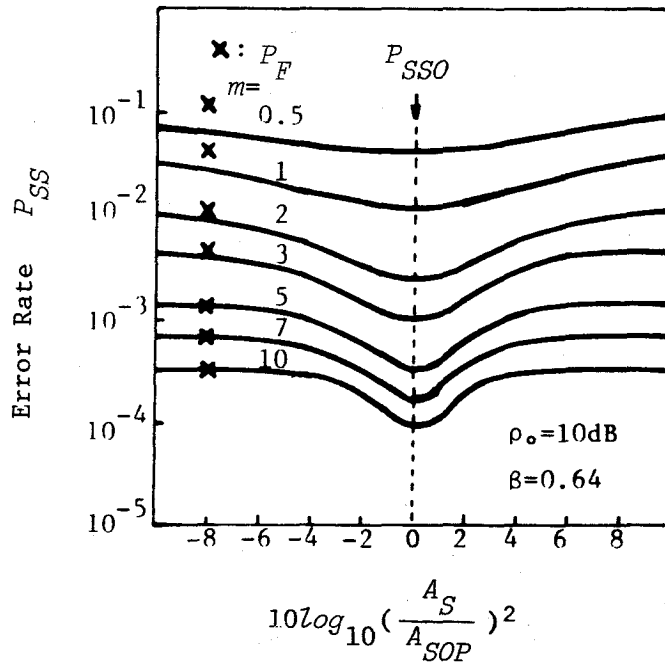


Fig. 5.2 Effects of Offset from
Optimum Switching Level.

## 5.3.2 Postdetection Diversity

The postdetection diversity techniques have two kinds of strategies: a)two output components of the detectors are directly combined, b)two appropriately weighted output components are combined. Though the latter has greater improvement effects on performance compared with the former, the simpliness of the implementation confines the analysis of this thesis to the former strategy.

The probability density function of the two output components for the mark signal, $p(V_1|\dot{\psi}_o=\Delta\omega_d,r_1)$ and $p(V_2|\dot{\psi}_o=\Delta\omega_d,r_2)$, are given after replacing $r$ with $r_1$ and $r_2$ in (4.10) and (4.13). Since the input noise components are uncorrelated, the probability density function of the combined output $p(V|\dot{\psi}_o=\Delta\omega_d,r_1,r_2)$ can be obtained by the convolution as follows:

$$p(V|\dot{\psi}_o=\Delta\omega_d,r_1,r_2)=p(V_1|\dot{\psi}_o=\Delta\omega_d,r_1)$$
$$\otimes p(V_2|\dot{\psi}_o=\Delta\omega_d,r_2) \ . \tag{5.9}$$

Then, the error rate for the postdetection diversity $P_P$ is given by

$$P_P = \int_{-\infty}^{0} dV \int_{0}^{\infty} dr_1 \int_{0}^{\infty} dr_2\, p(r_1,r_2)p(V|\dot{\psi}_o=\Delta\omega_d,r_1,r_2) \ . \tag{5.10}$$

The joint probability density function of $r_1$ and $r_2$, $p(r_1,r_2)$, necessary to derive $P_P$ in the $m$-distributed fading environments, is given as [22]

$$p(r_1,r_2) = \frac{4m^{2m}(r_1r_2)^{2m-1}/\Gamma(m-0.5)}{\sqrt{\pi}\Gamma(m)\,[\Omega^2(1-k^2)]^m}$$

$$\cdot \int_{0}^{\pi} d\zeta\, \sin^{2m-2}\zeta\exp\left\{-\frac{m}{1-k^2}\left(\frac{r_1^2}{\Omega}+\frac{r_2^2}{\Omega}-\frac{2\sqrt{k^2}r_1r_2\cos\zeta}{\Omega}\right)\right\} \ .$$

$$\tag{5.11}$$

The substitution of (5.9) and (5.11) into (5.10) yields the final result:

$$P_P = P_{P1} + 2P_{P2} + P_{P3} + 2P_{P4} \quad , \tag{5.12}$$

$$P_{Pi} = \int_0^{\frac{\pi}{2}} d\zeta \int_0^{\pi} d\chi \cdot \frac{C_i \, m^{2m} (\cos\zeta\sin\chi)^{2m-1} \sin^{2m-2}\chi}{\sqrt{\pi}\,\Gamma(m)\,\Gamma(m-0.5)(1-k^2)^m}$$

$$\left\{ \frac{\Gamma(2m)}{4D_i^{2m}} - \frac{\sqrt{\rho_o}\,\cos\zeta\sin\zeta\,\Gamma(2m+0.5)E_i}{\sqrt{2\pi}f_o(\beta)} \, (F_i+G_i)^{-(2m+\frac{1}{2})} \right.$$

$$\left. \cdot {}_2F_1\left(1, 2m+\frac{1}{2}; \frac{3}{2}; \frac{G_i}{F_i+G_i}\right) \right\} , \qquad (i=1,2,3,4)$$

$$\begin{cases} C_1 = 4 \\ C_2 = 2\beta \\ C_3 = \beta^2 \\ C_4 = \frac{\beta^2}{2} \end{cases} \qquad \begin{cases} D_1 = \frac{m}{1-k^2}(1-2\sqrt{k^2}\cos\zeta\sin\zeta\cos\chi) \\ D_2 = D_1 + \rho_o\cos^2\zeta \\ D_3 = D_1 + \rho_o \\ D_4 = D_1 + 2\rho_o\cos^2\zeta \end{cases}$$

$$\begin{cases} E_1 = \pi\beta \\ E_2 = \pi(\beta-1) \\ E_3 = \pi(\beta-2) \\ E_4 = \pi(\beta-2) \end{cases} \qquad \begin{cases} F_1 = F\pi^2\beta^2 \\ F_2 = F(\pi\beta-\pi)^2 \\ F_3 = F(\pi\beta-2\pi)^2 \\ F_4 = F(\pi\beta-2\pi)^2 \\ \quad F = \frac{2\rho_o\cos^2\zeta\sin^2\zeta}{f_o(\beta)} \end{cases}$$

where each term is explained as follows:

$P_{P1}$: the error rate due to the occurrence of no click on the two branches,

$P_{P2}$: the error rate due to the occurrence of one click on one of the two branches,

$P_{P3}$: the error rate due to the occurrence of one click on the both branches,

$P_{P4}$: the error rate due to the occurrence of two clicks on one of the two branches.

## 5.4 System Comparison

The numerical calculations of (5.1), (5.2), (5.6), (5.12) show the following results:

(1) Relation between the error rates and modulation indices (refer to Figs. 5.3 and 5.4).

1) As a whole, the smaller the correlation coefficient, the better the performance. When the input signals are uncorrelated, MRC has the best performance, EGC has the second best, SC has the third best, and SS has the lowest, except for the postdetection diversity.

2) Except for the postdetection diversity, it is seen that the inclination is negative for $\beta<0.6$, $\beta>1.8$ and positive for $0.6<\beta<1.8$. This can be explained as follows: a) For $\beta<0.6$, the probability that one click occurs in one digit duration is very small, so that the Gaussian noise is the main contributor to error. b) For $0.6<\beta<1.8$, an error occurs due to one click only. Especially, since the probability of the occurrence of one click is proportional to the modulation index, the inclination becomes positive. c) For $\beta>1.8$, although the average number of clicks increases, the contribution of clicks becomes smaller, as the modu-

lation index increases.  An error occurs due to the
interaction of the click and the Gaussian noise.
In the case of the postdetection diversity, the incli-
nation is negative for $\beta < 0.35$, $0.8 < \beta < 1.4$, $\beta > 1.7$, and
positive for $0.35 < \beta < 0.8$, $1.4 < \beta < 1.7$.  This can be ex-
plained as follows: i) For $\beta < 0.35$, it is identical to a)
described above.  ii) For $0.35 < \beta < 0.8$, it is identical
to b).  iii) For $0.8 < \beta < 1.4$, it is identical to c).
iv) For $1.4 < \beta < 1.7$, an error occurs  due to two
clicks.  Especially, since the probability of the occur-
rence of two clicks is proportional to $\beta^2$, the inclina-
tion becomes positive.  v) For $\beta > 1.7$, it is identical
to c).

3) The optimum modulation index yielding the minimum
   error rate is found within an appropriate range of
   the modulation index.  This means that the increase
   of $\beta$ may not necessarily improve the performance of
   the system because more noise may be introduced.
   Except for the postdetection diversity, this optimum
   modulation index becomes about 0.6 and it is not
   affected by the types of diversity, values of average
   input CNR, values of fading figure, or values of
   correlation coefficient.  In the case of postdetection
   diversity, this optimum point is about 0.35 for $\beta < 1$,
   and 1.4 for $\beta < 2$.

4) In the region of $m=1$, $0.36 < \beta < 1.4$ and of $m=5$, $0.46 < \beta < 1$,
   the error rate for the postdetection diversity is
   greater than that for no diversity.

5) In the case of the postdetection diversity, the effect
   of the correlation between two branches becomes smaller
   than the case of MRC.  Especially, for $0.4 < \beta < 1$, there
   is no difference between the case of $k=0$ and that of

$k$=0.9.  This can be explained as follows: In this
region of β, since only one click on a single branch
is the main contributor, the occurrence of clicks on
the other branch does not affect the error rate.
That is, in the case of the postdetection diversity,
the worse branch dominates the error rate performance.
On the other hand, in the case of the predetection
diversity, the better branch dominates the error rate
performance.

(2) Relations between error rates and fading figures
    (refer to Fig. 5.5).

  1) As $m$ increases (fading becomes shallower), the
     difference between the improvement effect of EGC and
     that of SS becomes greater.  On the other hand, MRC
     and EGC give nearly identical performances; SC and SS
     so do.

  2) For $m$=0.5 (one-sided Gaussian), SC yields the same
     error rate as EGC does.

(3) Relations between error rates and average input CNRs
    (refer to Fig. 5.6).

  1) As the average CNR increases, the error rate decreases.
     Furthermore, the degree of this decrease becomes
     greater, as $m$ increases.
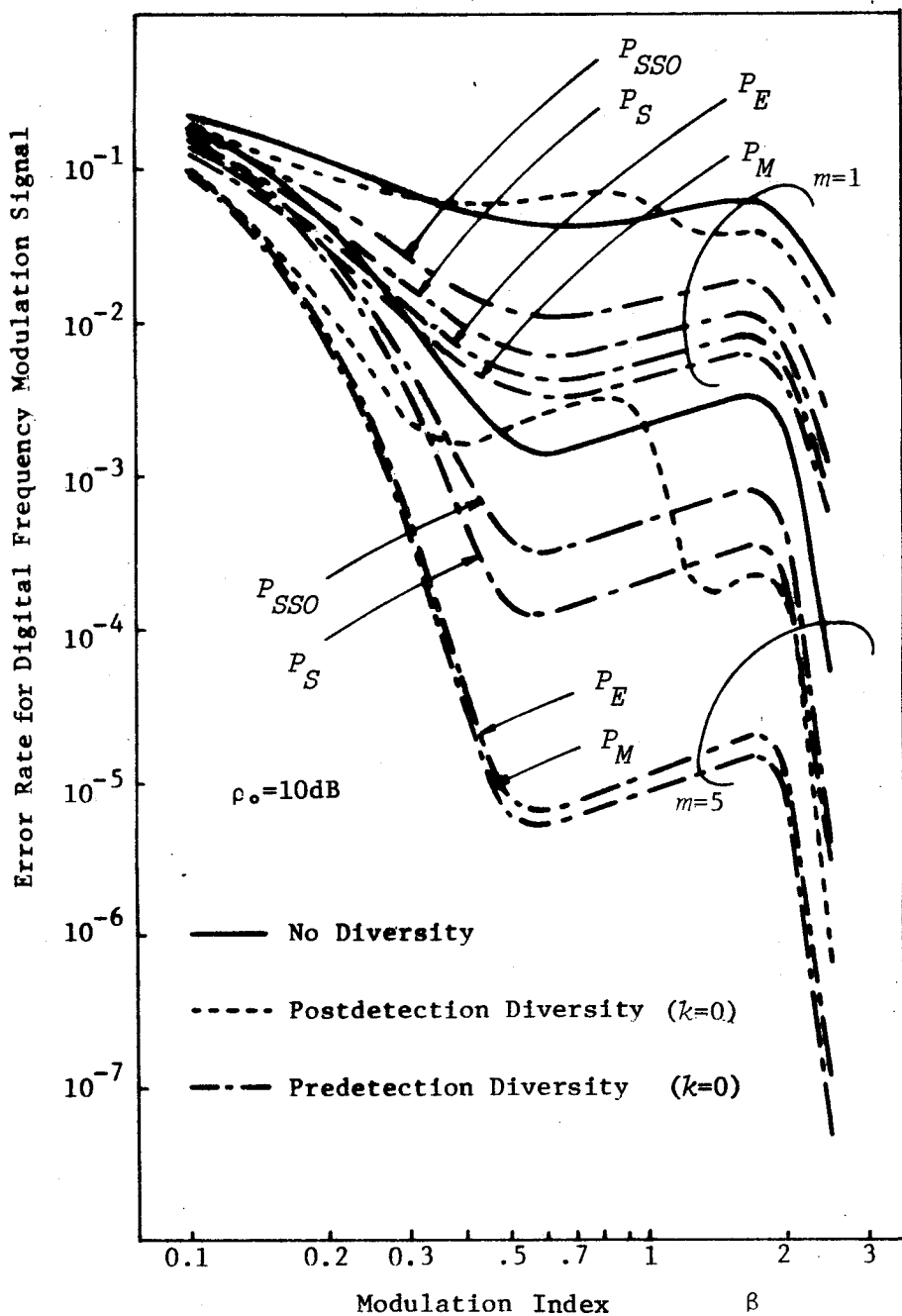
Fig. 5.3  Error Rates vs. Modulation Indices.

- 49 -
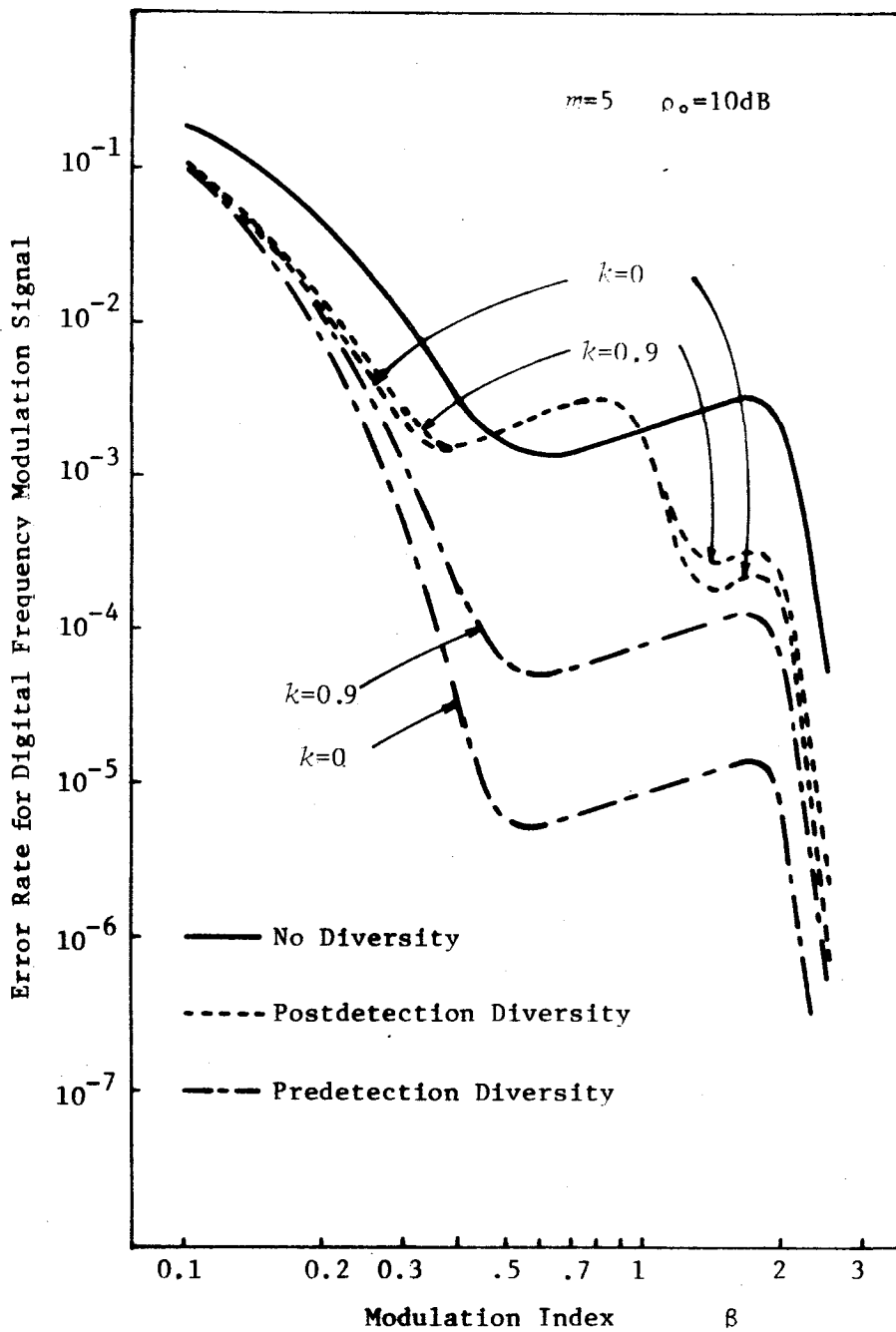
Fig. 5.4   Error Rates vs. Modulation Indices.
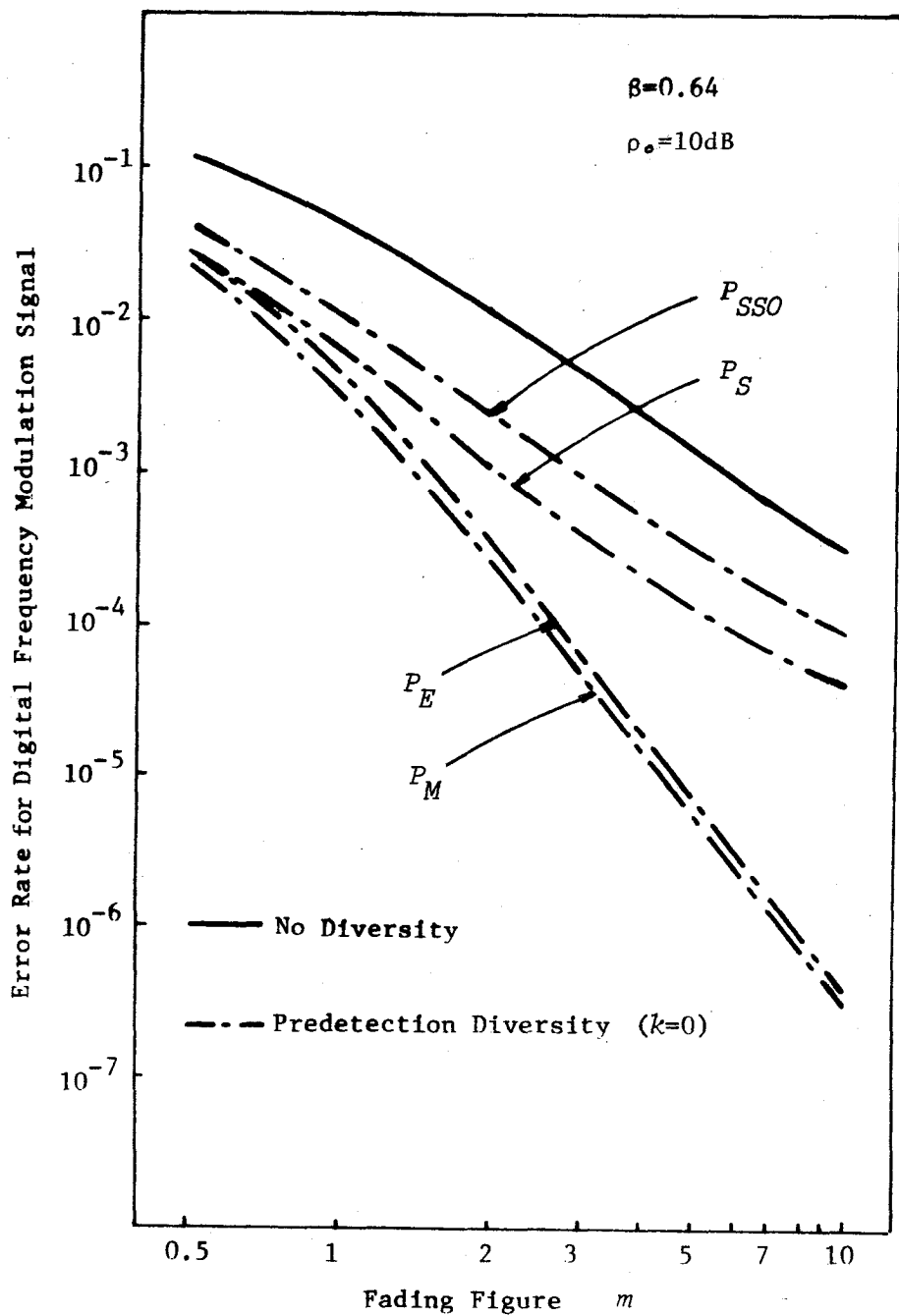
Fig. 5.5  Error Rates vs. Fading Figures.
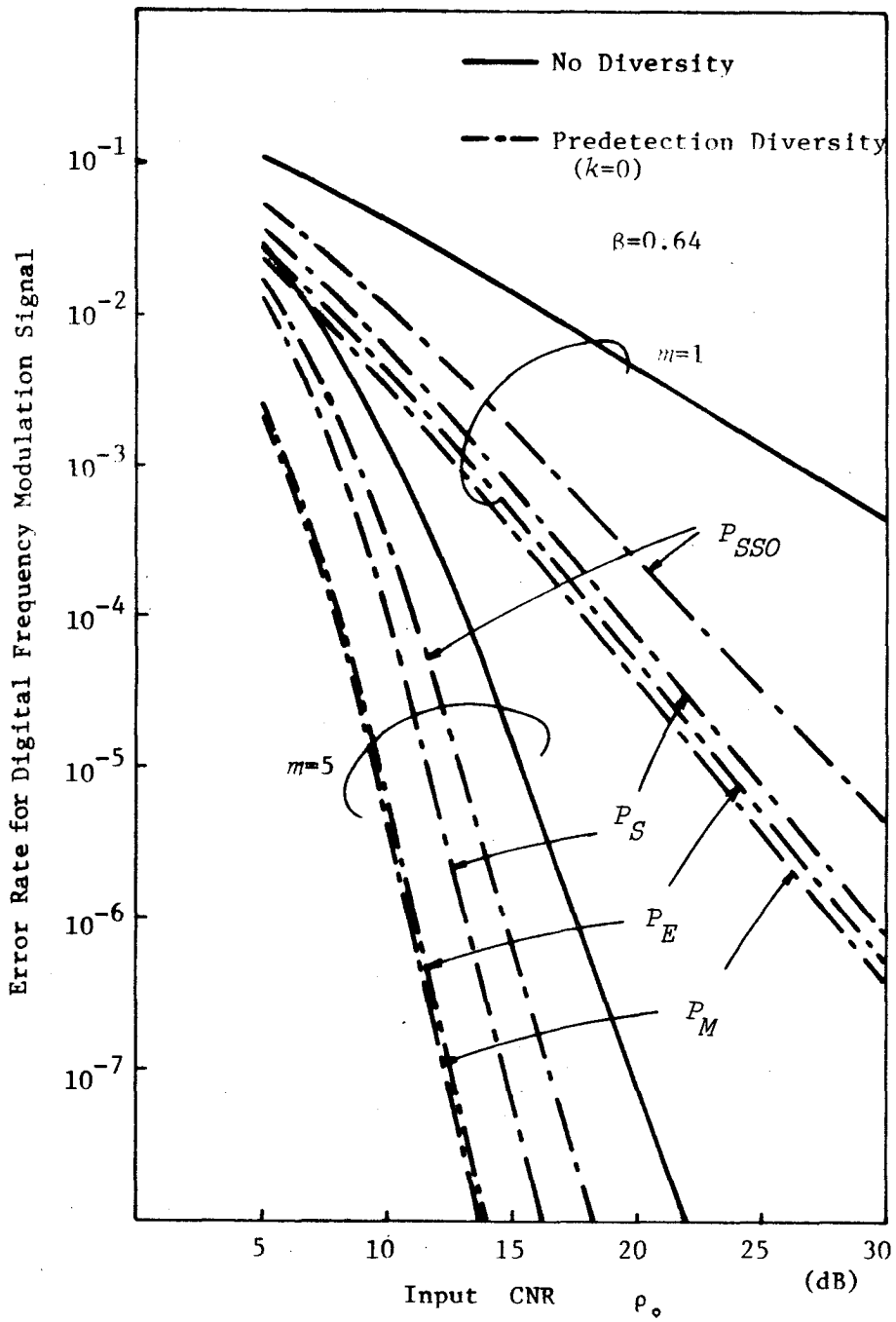
Fig. 5.6   Error Rates vs. Input CNRs.

## 5.5 Concluding Remarks

In this chapter, the error rate characteristics of the digital FM system in the nonselective $m$-distributed fading environments have been described including the improvement effects owing to the predetection and the postdetection diversity techniques. Furthermore, for the Switch-and-Stay diversity, a design method of an optimum switching level attaining a minimum error rate has been shown.

The main results obtained are summarized as follows:

(1) The optimum modulation index yielding the minimum error rate is found within an appropriate range of the modulation index. Furthermore, except for the postdetection diversity, the value of this optimum index is not affected by the types of diversity, values of average input CNR, values of fading figure, and values of correlation coefficient.

(2) The better branch dominates the error rate performance for the predetection diversity. On the other hand, the worse branch dominates the error rate performance for the postdetection diversity.

Chapter 6

DIGITAL PHASE-FREQUENCY
MODULATION SYSTEM  [62]


6.1  Introductory Remark

Hybrid modulation schemes have been achieved with the
combination of phase and amplitude [63]-[68].  However, when
these signals pass through a nonlinear device like a travelling
wave tube operating in the saturation region, the information
in the amplitude will be lost. On the other hand, the hybrid
modulation in terms of phase shift keying and frequency shift
keying can be amplified without loss of its information by
such a device.  This chapter proposes a new hybrid modulation
named "digital phase-frequency modulation (PFSK[†]: Phase-
Frequency Shift Keying)", in which the multilevel transmission
can be performed by the phase-frequency combination, and its
error rate and power spectral density are given.

Five kinds of noncoherent detection system are proposed.
They can include a delay detector, a frequency discriminator,
and an integrate-and-dump filter.  When detected by the dis-
criminator, the impulse noise appears at the output, because
this PFSK signal has a sharp phase shift which includes phase
information.  Furthermore, the limitation of the bandwidth
enhances the effect of this noise.  Therefore, one of the
proposed systems is implemented to reduce the effect of this
impulse noise.

---

[†]  In this thesis, the term "PFSK" is used to mean "digital
phase-frequency modulation" for the sake of expressional
simplicity.

## 6.2 Signal Configuration

The PFSK signal has two bits consisting of phase information and frequency information in one digit duration $T$, and is expressed as

$$s_k(t) = r \cos [\omega_0 t + \sum_{l=-\infty}^{k-1} (a_l - \frac{1}{2}) 2\pi + (a_k - \frac{1}{2}) \frac{2\pi}{T} (t-kT)$$

$$+ \sum_{l=-\infty}^{k-1} b_l \pi + b_k \pi + \theta] , \qquad kT \le t \le (k+1)T \qquad (6.1)$$

$$a_k, b_k = \begin{cases} 1, & \text{"mark"} \\ 0, & \text{"space"} \end{cases} \qquad \begin{array}{c} \omega_0 T = 2m\pi \\ (m : \text{integer}) \end{array}$$

where $a_k$ represents frequency information, $b_k$ phase information.

## 6.3 Detection System

Five PFSK noncoherent detection systems will be proposed in this section. These detection systems can include a delay detector (Fig. 6.1), a frequency discriminator, and an integrate-and-dump filter. In Fig. 6.2, the phase variation of the PFSK signal and the behavior of the detector outputs are illustrated.
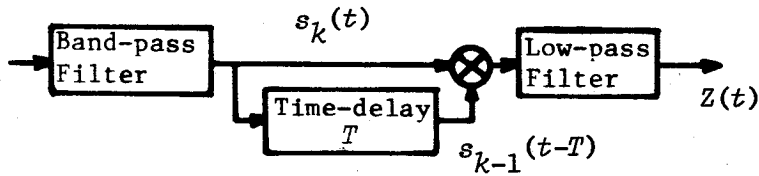


Fig. 6.1  Delay Detector.
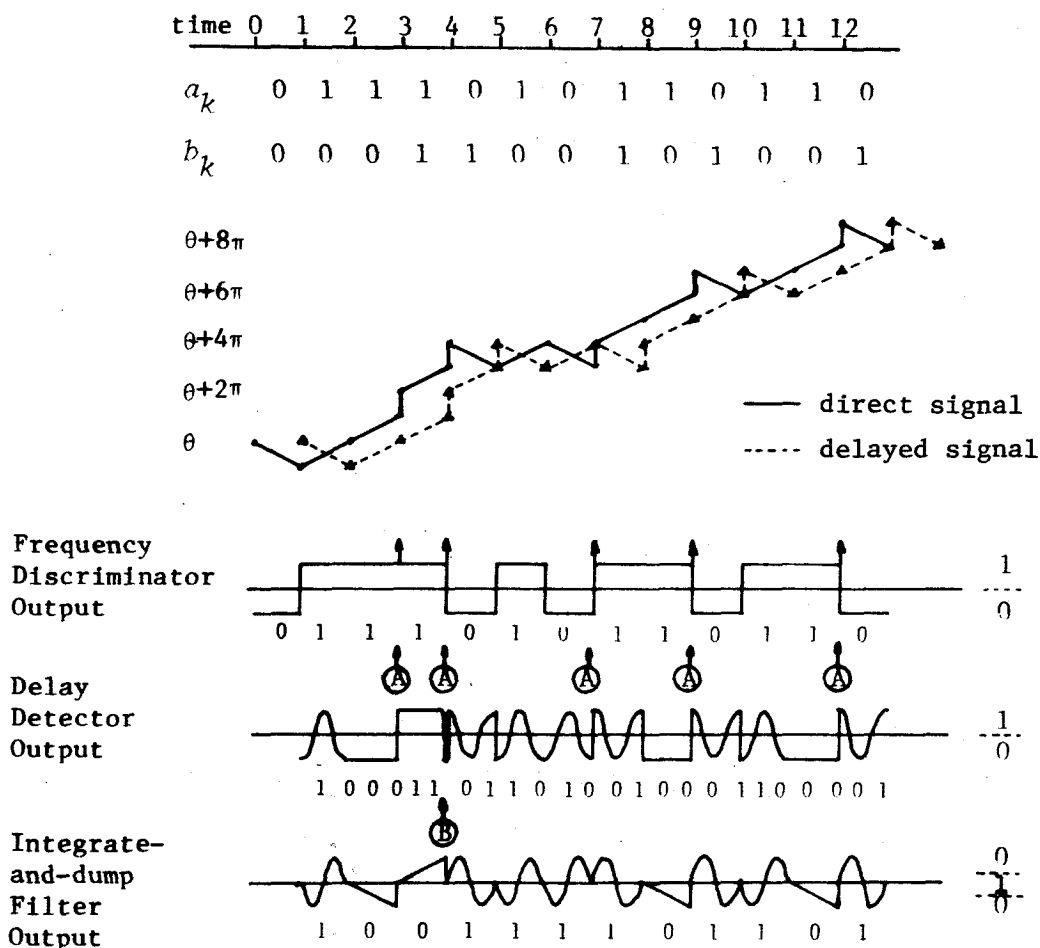
Fig. 6.2 Digital Phase-Frequency Modulation Signal
and Behavior of Detector Outputs.

The output of the delay circuit $s_{k-1}(t-T)$ is represented
by

$$s_{k-1}(t-T) = r\cos[\omega_o(t-T) + \sum_{l=-\infty}^{k-2}(a_l - \frac{1}{2})2\pi$$

$$+(a_{k-1}-\frac{1}{2})\frac{2\pi}{T}(t-kT) + \sum_{l=-\infty}^{k-2}b_l\pi + b_{k-1}\pi + \theta] . \qquad (6.2)$$

Then the output of the low-pass filter, $Z(t)$, becomes

$$Z(t) = LPF[s_k(t) \cdot s_{k-1}(t-T)]$$

$$= \frac{r^2}{2}\cos[\omega_o T + (a_{k-1}-\frac{1}{2})2\pi + (a_k - a_{k-1})\frac{2\pi}{T}(t-kT) + b_k\pi] , \qquad (6.3)$$

where $LPF[\cdot]$ denotes the operation of taking a low frequency component. When sampled at the end of the digit $t=(k+1)T$, its sampled value $Z[(k+1)T]$ is given by

$$Z[(k+1)T] = \frac{r^2}{2}\cos[\omega_o T + (a_k - \frac{1}{2})2\pi + 2\pi(a_k - a_{k-1}) + b_k\pi]$$

$$= -\frac{r^2}{2}\cos b_k\pi . \qquad (6.4)$$

Therfore, it is seen that the delay detector may recover the phase information $b_k$. Furtheremore, the other value sampled at $t=(k+\frac{1}{2})T$, $Z[(k+\frac{1}{2})T]$, is represented by

$$Z[(k+\frac{1}{2})T] = -\frac{r^2}{2}\cos[(a_k - a_{k-1} + b_k)\pi]$$

$$= -\frac{r^2}{2}\cos[(a_k \oplus a_{k-1} \oplus b_k)\pi] , \qquad (6.5)$$

where "$\oplus$" denotes the operation of modulo 2 addition. The above equation means that the knowledge of the phase information $b_k$ can determine the difference of the frequency information $a_k \oplus a_{k-1}$, and vice versa.

The block diagrams of the proposed five systems are shown in Fig. 6.3, where $c_k$ represents the information sampled at $t=(k+\frac{1}{2})T$ and also takes the value of 1 or 0.
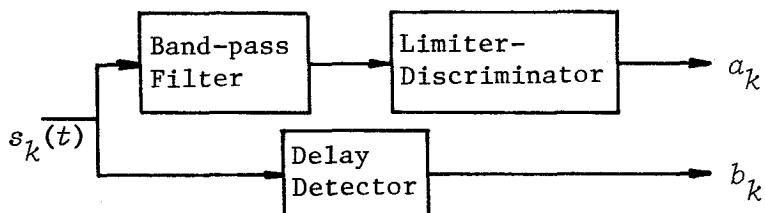


a) System 1.
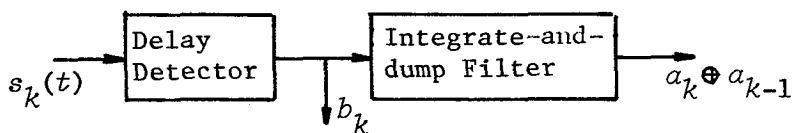


b) System 2.
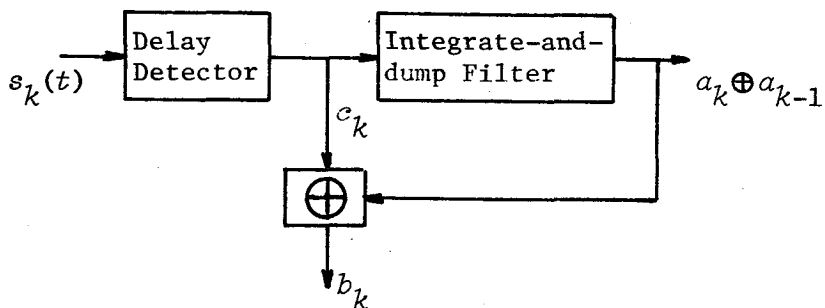


c) System 3.
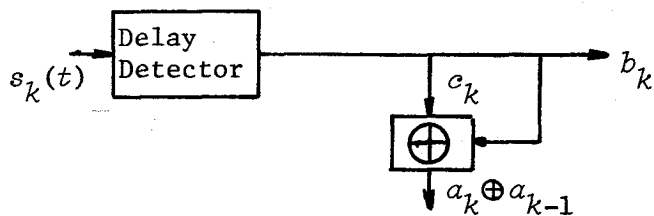
d) System 4.
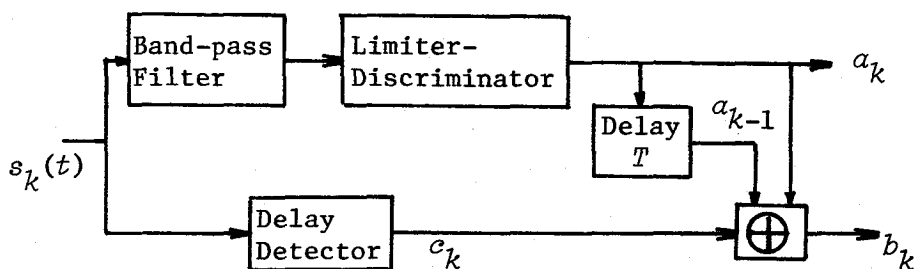


e) System 5.

Fig. 6.3  Detection Systems for Digital
Phase-Frequency Modulation Signal.

## 6.4  Some Comments on Detection System

The sharp phase shift, which the phase information
generates at the transient point, results in the impulse noise
at the frequency discriminator output.  This impulse noise is
caused by the differentiating operation of the discriminator
and appears at point ⒶA in Fig. 6.2.  Though the impulse is
illustrated like the delta function for convenience, in prac-
tice, the time duration of interest is about two times as wide

as the reciprocal of the BPF bandwidth [6, p.329]. For example, if the BPF bandwidth is defined, following Carson's rule, as

$$2B = 2(1+\beta)\frac{1}{2T} = \frac{2}{T}, \qquad (6.6)$$

then the time duration becomes $T$ sec. Therefore, only the midpoint of the digit is not affected so much by the impulses, so that the frequency discriminator output is sampled at $t=(k+\frac{1}{2})T$ in systems 1 and 5.

The impulse observed at point Ⓑ, due to the simultaneous phase shift of the direct signal and the delayed signal, also affects the output of the delay detector in the vicinity of the transient point. Especially, the limitation of BPF bandwidth enlarges its influence. However, as discussed on the impulse at the discriminator output, the midpoint of the digit is not affected so much.

Systems 1-4 can be adopted under the assumption that the effects of the above impulses may be neglected, while system 5 is composed by the consideration of the small effects of the impulses at the midpoint of the digit.

From the viewpoint of the way to recover the information, in systems 1 and 2, the frequency information and the phase information can be obtained independently. On the other hand, systems 3-5 are the composite detection systems which utilize the information $c_k$ due to the combination of $a_k$ and $b_k$. Therefore, the error of $a_k$ affects $b_k$, and the error of $b_k$ affects $a_k$: error-propagation phenomenon occurs.

From the viewpoint of the complexity of the implementation, system 4 is the simplest and system 5 is the most complicated.

## 6.5 Error Rate

System 1, which recovers the information by means of detecting the frequency and phase-difference components, is the most straightforward one and its error rate can be easily obtained under the assumption that the effects of the impulses may be neglected.

The error rate of the frequency information $P_{EF}$ is derived by Bennet [35], and given by

$$P_{EF} = \frac{1}{2}\,\text{erfc}\sqrt{\rho} + \frac{\sqrt{\rho}}{2\sqrt{\pi}} \int_{-1}^{1} e^{-\rho x^2}\,\text{erfc}(d\sqrt{\rho(1-x^2)}\,)\,dx \quad, \qquad (6.7)$$

where $\rho$ is the input CNR. The term $d$ is defined by

$$d = \frac{\pi}{\alpha T} \quad, \qquad\qquad\qquad (6.8)$$

where $\alpha$ is the r.m.s. bandwidth given in (2.20).

The error rate of the phase information $P_{EP}$ can be derived as follows. Defining the input noise $n(t)$ as

$$n(t) = \xi(t)\cos\omega_0 t - \eta(t)\sin\omega_0 t \quad, \qquad\qquad (6.9)$$

the sums of the signal and noise, $e_k(t)$ and $e_{k-1}(t-T)$, are given as follows:

$$e_k(t) = [r\cos\{ \sum_{l=-\infty}^{k-1} (a_l - \frac{1}{2})\,2\pi + (a_k - \frac{1}{2})\frac{2\pi}{T}(t-kT)$$

$$+ \sum_{l=-\infty}^{k-1} b_l \pi + b_k \pi + \theta \} + \xi(t)\,]\cos\omega_0 t$$

$$-[r\sin\{\sum_{l=-\infty}^{k-1}(a_l-\frac{1}{2})2\pi+(a_k-\frac{1}{2})\frac{2\pi}{T}(t-kT)$$

$$+\sum_{l=-\infty}^{k-1}b_l\pi+b_k\pi+\theta\}+n(t)]\sin\omega_o t \quad , \tag{6.10}$$

$$e_{k-1}(t-T)=[r\cos\{\sum_{l=-\infty}^{k-2}(a_l-\frac{1}{2})2\pi+(a_{k-1}-\frac{1}{2})\frac{2\pi}{T}(t-kT)$$

$$+\sum_{l=-\infty}^{k-2}b_l\pi+b_{k-1}\pi+\theta\}+\xi(t-T)]\cos\omega_o t$$

$$-[r\sin\{\sum_{l=-\infty}^{k-2}(a_l-\frac{1}{2})2\pi+(a_{k-1}-\frac{1}{2})\frac{2\pi}{T}(t-kT)$$

$$+\sum_{l=-\infty}^{k-2}b_l\pi+b_{k-1}\pi+\theta\}+n(t-T)]\sin\omega_o t \ . \tag{6.11}$$

At the sampling instant $t=(k+1)T$, the output $Z[(k+1)T]$ becomes

$$Z[(k+1)T]=\frac{1}{2}(P_1 P_2+Q_1 Q_2) \ , \tag{6.12}$$

$$\begin{cases} P_1=r\cos\chi_k+\xi_1 \\ P_2=r\cos\chi_{k-1}+\xi_2 \\ Q_1=r\sin\chi_k+n_1 \\ Q_2=r\sin\chi_{k-1}+n_2 \end{cases}$$

$$\chi_k=\sum_{l=-\infty}^{k}(a_l-\frac{1}{2})2\pi+\sum_{l=-\infty}^{k}b_l\pi+\theta$$

where the subscripts "1" and "2" in $\xi$ and $n$, correspond to the time instants $(k+1)T$ and $kT$, respectively. The above equation is also represented by another form:

$$Z[(k+1)T] = \frac{1}{8}[\{(P_1+P_2)^2+(Q_1+Q_2)^2\}-\{(P_1-P_2)^2+(Q_1-Q_2)^2\}] \ .$$

$$(6.13)$$

The probability density function for the output signal  
$Z[(k+1)T]$, leads to the derivation of the error rate $P_{EP}$ .  
Under the assumption that the probability of the occurrence of  
"0" and "1" are equally likely, the decision of the transmitted  
data is based on the sign of equation within the bracket, so  
that the following discussion takes interest only in equation  
within the bracket.

Let $u_1$, $u_2$, $v_1$, $v_2$ be defined as follows:

$$
\begin{aligned}
u_1 &= P_1 + P_2 & u_2 &= P_1 - P_2 \\
v_1 &= Q_1 + Q_2 & v_2 &= Q_1 - Q_2 \ .
\end{aligned}
$$

$$(6.14)$$

Since $P_1$, $P_2$, $Q_1$, $Q_2$ are Gaussian distributed, the transformed  
variables $u_1$, $u_2$, $v_1$, $v_2$ are also Gaussian distributed.  Their  
means and variances are given as follows:

$$
\begin{aligned}
\overline{u_1} &= r\cos\chi_k + r\cos\chi_{k-1} \\
\overline{u_2} &= r\cos\chi_k - r\cos\chi_{k-1} \\
\overline{v_1} &= r\sin\chi_k + r\sin\chi_{k-1} \\
\overline{v_2} &= r\sin\chi_k - r\sin\chi_{k-1} \ ,
\end{aligned}
$$

$$(6.15)$$

$$
\left.
\begin{aligned}
&\overline{\xi_1^2} = \overline{\xi_2^2} = \overline{\eta_1^2} = \overline{\eta_2^2} = \sigma_n^2 \\[4pt]
&\overline{\xi_1\xi_2} = \overline{\xi_1\eta_1} = \overline{\xi_1\eta_2} = \overline{\xi_2\eta_1} = \overline{\xi_2\eta_2} = \overline{\eta_1\eta_2} = 0 \\[4pt]
&\overline{(u_1-\overline{u_1})^2} = \overline{(u_2-\overline{u_2})^2} = \overline{(v_1-\overline{v_1})^2} = \overline{(v_2-\overline{v_2})^2} = 2\sigma_n^2
\end{aligned}
\right\}
\quad (6.16)
$$

$$\overline{(u_1 - \overline{u}_1)(v_1 - \overline{v}_1)} = \overline{(u_1 - \overline{u}_1)(u_2 - \overline{u}_2)} = \overline{(u_2 - \overline{u}_2)(v_2 - \overline{v}_2)}$$

$$= \overline{(v_1 - \overline{v}_1)(v_2 - \overline{v}_2)} = \overline{(u_1 - \overline{u}_1)(v_2 - \overline{v}_2)} = \overline{(u_2 - \overline{u}_2)(v_1 - \overline{v}_1)} = 0 \quad ,$$

where "$\overline{\cdot}$" denotes the operation of taking the ensemble average. Therefore, the new variables are uncorrelated each other, so that $u_1$ and $v_1$ (or $u_2$ and $v_2$) can be regarded as the inphase and quadrature components of narrow band Gaussian process. Moreover, defining $R_1$ and $R_2$ as

$$R_1 = \sqrt{u_1^2 + v_1^2} \quad , \qquad R_2 = \sqrt{u_2^2 + v_2^2} \quad , \tag{6.17}$$

their probability density functions, $p(R_1)$ and $p(R_2)$, are expressed by

$$p(R_1) = \frac{R_1}{2\sigma_n^2} I_0 \left( \frac{\sqrt{B_1}\, R_1}{2\sigma_n^2} \right) \exp\left( - \frac{R_1^2 + B_1}{4\sigma_n^2} \right) ,$$

$$\tag{6.18}$$

$$p(R_2) = \frac{R_2}{2\sigma_n^2} I_0 \left( \frac{\sqrt{B_2}\, R_2}{2\sigma_n^2} \right) \exp\left( - \frac{R_2^2 + B_2}{4\sigma_n^2} \right) ,$$

where

$$B_1 = \overline{u}_1^2 + \overline{v}_1^2 = 2r^2 - 2r^2 \cos b_k \pi \quad ,$$

$$\tag{6.19}$$

$$B_2 = \overline{u}_2^2 + \overline{v}_2^2 = 2r^2 + 2r^2 \cos b_k \pi \quad .$$

The error rate $P_{EP}$ is determined by

$$P_{EP} = prob\,(P_1 P_2 + Q_1 Q_2 < 0 \,|\, b_k = 1)$$

$$= prob\,(R_1 < R_2 \,|\, b_k = 1)$$

$$= prob(P_1 P_2 + Q_1 Q_2 > 0 | b_k = 0)$$

$$= prob(R_1 > R_2 | b_k = 0) \quad . \tag{6.20}$$

When $b_k = 1$, the probability density functions, $p(R_1)$ and $p(R_2)$, become

$$p(R_1) = \frac{R_1}{2\sigma_n^2} I_0 \left( \frac{r R_1}{2\sigma_n^2} \right) \exp\left( - \frac{R_1^2 + 4r^2}{4\sigma_n^2} \right) ,$$

$$\tag{6.21}$$

$$p(R_2) = \frac{R_2}{2\sigma_n^2} \exp\left( - \frac{R_2^2}{4\sigma_n^2} \right) \quad .$$

The utilization of (6.21) and (A.6) in Appendix A, derives the error rate $P_{EP}$ for the phase information:

$$P_{EP} = \int_0^\infty dR_1 p(R_1) \{ \int_{R_1}^\infty dR_2 p(R_2) \} = \frac{1}{2} \exp\left( - \frac{r^2}{2\sigma_n^2} \right)$$

$$= \frac{1}{2} e^{-\rho} \quad . \tag{6.22}$$

It is interesting to note that (6.22) is the same as the error rate for DPSK [48, p. 254].

Fig. 6.4 shows the power spectral density of the PFSK signal with that of the DPSK signal. From this figure, it is seen that the main lobe is one and a half times wider than that of DPSK signal. However, the PFSK signal has two bits per one time duration $T$, whereas the DPSK signal has one bit per the same duration. Thus it may be said that the width of main lobe per one bit information is compressed in the PFSK signaling.
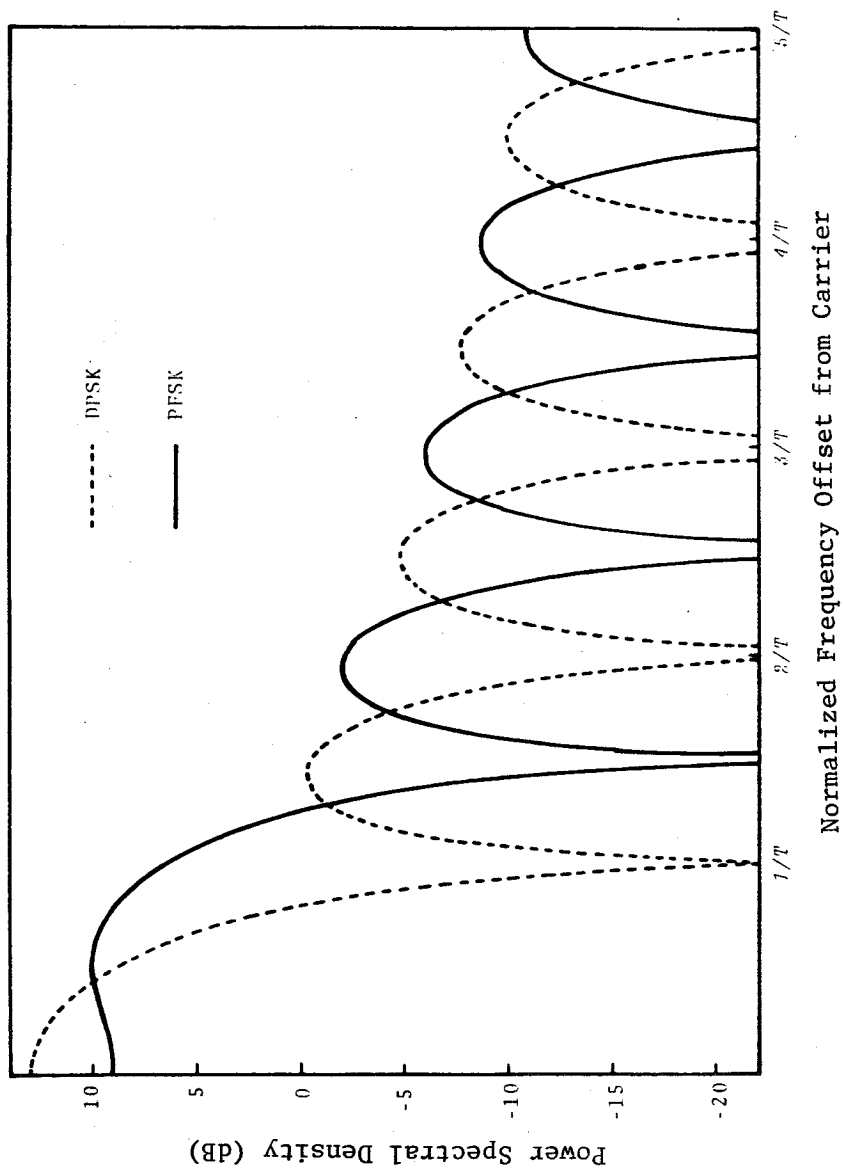
Fig. 6.4 Power Spectral Density for PFSK and DPSK.

- 66 -

## 6.6 Concluding Remarks

In this chapter, a new hybrid modulation signaling named PFSK has been proposed, and its detection system, power spectral density, and error rate have been discussed. The following chapter extends the analysis described in this chapter to the case where the input PFSK signal is subject to fading.

In addition, it is interesting to note that the concept of this PFSK signaling leads to the hybrid modulation scheme by the combination of amplitude, phase, and frequency shift keyings.

Chapter 7

# DIGITAL PHASE-FREQUENCY MODULATION
# SYSTEM IN FADING ENVIRONMENTS

## 7.1 Introductory Remark

In land mobile radio communication systems, the propaga-
tion between a base station and a vehicle is usually performed
not only by a direct line-of-sight route, but via multiple
random paths because of reflection, scattering, and diffrac-
tion. Therefore, in the case of UHF or microwave land mobile
radios, rapid and deep fading phenomenon called time-selective
fading will occur on the received signal when a vehicle moves
through an interference field composed of many waves. A re-
ceived signal suffering from such a fading phenomenon has a
Rayleigh distributed envelope and uniformly distributed phase
[23, Ch. 1].

In this chapter, the error rate characteristics of the
PFSK signal proposed in the foregoing chapter are discussed
when utilized in the nonselective $m$-distributed fading envi-
ronment and the time-selective Rayleigh fading environment.
Especially, in the latter case of the fading environment, the
difference between the effect of fading on the phase informa-
tion and that on the frequency information is described.

## 7.2 Error Rate in Nonselective Fading

The error rate for the PFSK signal in the nonselective
$m$-distributed fading environments can be derived by a similar
method as in Sec. 5.2. Averaging (6.7) and (6.22) over $r$,
the corresponding error rates $P_{EFS}$ and $P_{EPS}$ are given by

$$P_{EFS} = \int_0^\infty P_{EF}\, p(r)\, dr$$

$$= \frac{1}{2} - \frac{\Gamma(m+0.5)\sqrt{\rho_o}}{\sqrt{\pi}\,\Gamma(m)\sqrt{m}}\,(1+\frac{\rho_o}{m})^{-(m+\frac{1}{2})}\, {_2F_1}(1,m+\frac{1}{2};\frac{3}{2};\frac{\rho_o}{m+\rho_o})$$

$$+ \int_0^\infty dx\, \frac{m^m\Gamma(m+0.5)\sqrt{\rho_o}}{2\sqrt{\pi}\,\Gamma(m)}\left\{m+x^2\rho_o\right\}^{-(m+0.5)}$$

$$- \frac{m^m\sqrt{3(1-x^2)}\,\Gamma(m+1)\rho_o}{2\pi\Gamma(m)}\left\{x^2\rho_o+m+0.75\rho_o(1-x^2)\right\}^{-(m+1)}$$

$$\cdot\, {_2F_1}(1,m+1;\frac{3}{2};\frac{0.75\rho_o(1-x^2)}{m+x^2\rho_o+0.75\rho_o(1-x^2)})\ , \tag{7.1}$$

$$P_{EPS} = \int_0^\infty P_{EP}\, p(r)\, dr$$

$$= \frac{m^m}{2(\rho_o+m)^m}\ . \tag{7.2}$$

## 7.3  Error Rate in Time-Selective Fading

The input signal subject to the time-selective (fast) Rayleigh fading encountered in the typical UHF or microwave land mobile radio channels, can be represented as

$$s_k(t) = X(t)\cos\{\omega_o t+\lambda_k(t)\}-Y(t)\sin\{\omega_o t+\lambda_k(t)\}\ , \tag{7.3}$$

$$\lambda_k(t) = \sum_{l=-\infty}^{k-1}(a_l-\frac{1}{2})2\pi+(a_k-\frac{1}{2})\frac{2\pi}{T}(t-kT)$$

$$+\sum_{l=-\infty}^{k-1}b_l\pi+b_k\pi\ , \qquad kT\le t\le(k+1)T$$

where $X(t)$ and $Y(t)$ are statistically independent Gaussian processes of zero mean value and of variance $\sigma_c^2$.

When system 1 (as described in Sec. 6.3) is utilized, the error rate of the frequency information $P_{EFF}$ is given by Hirade [25] under the assumption that the Doppler spectrum is symmetric about the carrier frequency:

$$P_{EFF} = \frac{1}{2}\left\{ 1 - \frac{2\pi\Delta f_d \, \rho_o}{\sqrt{(\rho_o+1)\{-\rho_o \ddot{\rho}_X(0) - \ddot{\rho}_\xi(0) + (2\pi\Delta f_d)^2 \rho_o\}}} \right\} \ , \quad (7.4)$$

$$-\ddot{\rho}_X(0) = \frac{4\pi^2}{\sigma_c^2} \int_{-\infty}^{\infty} f^2 S_X(f)\,df \ ,$$

$$-\ddot{\rho}_\xi(0) = \frac{4\pi^2}{\sigma_n^2} \int_{-\infty}^{\infty} f^2 S_\xi(f)\,df \ ,$$

where $S_X(f)$ is the two-sided power spectral density of $X(t)$, and $S_\xi(f)$ is that of $\xi(t)$.

The procedure to derive the error rate $P_{EPF}$ is the same as in Sec. 6.5. The outputs $e_k(t)$ and $e_{k-1}(t-T)$ corresponding to (6.10) and (6.11) are represented by

$$e_k(t) = [X(t)\cos\lambda_k(t) - Y(t)\sin\lambda_k(t) + \xi(t)]\cos\omega_o t$$

$$- [X(t)\sin\lambda_k(t) + Y(t)\cos\lambda_k(t) + \eta(t)]\sin\omega_o t, \quad (7.5)$$

$$e_{k-1}(t-T) = [X(t-T)\cos\lambda_{k-1}(t-T) - Y(t-T)\sin\lambda_{k-1}(t-T)$$

$$+ \xi(t-T)]\cos\omega_o t$$

$$- [X(t-T)\sin\lambda_{k-1}(t-T) + Y(t-T)\cos\lambda_{k-1}(t-T)$$

$$+ \eta(t-T)]\sin\omega_o t \ . \quad (7.6)$$

Therefore, the output of the LPF at the sampling instant, $Z[(k+1)T]$, becomes

$$Z[(k+1)T] = \frac{1}{2}(P_1 P_2 + Q_1 Q_2) , \tag{7.7}$$

$$
\begin{cases}
P_1 = X_1 \cos\chi_k - Y_1 \sin\chi_k + \xi_1 \\[1em]
P_2 = X_2 \cos\chi_{k-1} - Y_2 \sin\chi_{k-1} + \xi_2 \\[1em]
Q_1 = X_1 \sin\chi_k + Y_1 \cos\chi_k + \eta_1 \\[1em]
Q_2 = X_2 \sin\chi_{k-1} + Y_2 \cos\chi_{k-1} + \eta_2 \\[1em]
\chi_k = \sum_{l=-\infty}^{k}(a_l - \frac{1}{2})2\pi + \sum_{l=-\infty}^{k} b_l \pi
\end{cases}
$$

where the subscripts "1" and "2" denotes the time instants $(k+1)T$ and $kT$ respectively. The random variables $X$ and $Y$ are Gaussian distributed and have the following relations:

$$\overline{X_1^2} = \overline{Y_1^2} = \overline{X_2^2} = \overline{Y_2^2} = \sigma_c^2$$

$$\overline{X_1 X_2} = \overline{Y_1 Y_2} = R_X(T) = \sigma_c^2 \rho_X(T) \tag{7.8}$$

$$\overline{X_1 Y_1} = \overline{X_2 Y_2} = \overline{X_1 Y_2} = \overline{X_2 Y_1} = 0 ,$$

where $\sigma_c^2$ is the average carrier power, and $\rho_X(T)$ is the normalized autocorrelation function of the inphase or quadrature component of the faded signal. The relation on $\xi_1$, $\xi_2$, $\eta_1$, $\eta_2$ are given in (6.16). Utilizing the relations in (6.16) and (7.8), the joint probability density function of the random variables $u_1$, $u_2$, $v_1$, $v_2$ given in (6.14) and (7.7), $p(u_1, u_2, v_1, v_2)$, is given by

$$p(u_1,u_2,v_1,v_2)= \frac{1}{(2\pi)^2(\alpha_0\beta_0-\gamma_0^2)}$$

$$\cdot \exp\left[-\frac{\beta_0(u_1^2+v_1^2)+\alpha_0(u_2^2+v_2^2)+2\gamma_0(u_2v_1-u_1v_2)}{2(\alpha_0\beta_0-\gamma_0^2)}\right] , \quad (7.9)$$

$$\alpha_0=2[\sigma_c^2+\sigma_n^2+\sigma_c^2\rho_X(T)\cos\{\chi_k-\chi_{k-1}\}] ,$$

$$\beta_0=2[\sigma_c^2+\sigma_n^2-\sigma_c^2\rho_X(T)\cos\{\chi_k-\chi_{k-1}\}] ,$$

$$\gamma_0=2\sigma_c^2\rho_X(T)\sin(\chi_k-\chi_{k-1}) .$$

Then the output signal $Z[(k+1)T]$ can be represented as

$$Z[(k+1)T]=\frac{1}{8}(R_1^2-R_2^2) , \quad (7.10)$$

through the following transformations:

$$u_1=R_1\cos\theta_1 \qquad v_1=R_1\sin\theta_1$$
$$\quad (7.11)$$
$$u_2=R_2\cos\theta_2 \qquad v_2=R_2\sin\theta_2 .$$

The joint probability density function of $R_1$ and $R_2$, $p(R_1,R_2)$, can be obtained as

$$p(R_1,R_2)= \int_0^{2\pi} d\theta_1 \int_0^{2\pi} d\theta_2 \, p(R_1,\theta_1,R_2,\theta_2)$$

$$= \frac{R_1R_2}{\alpha_0\beta_0-\gamma_0^2} \exp\left(-\frac{\beta_0R_1^2+\alpha_0R_2^2}{2(\alpha_0\beta_0-\gamma_0^2)}\right) I_0\left(\frac{\gamma_0R_1R_2}{\alpha_0\beta_0-\gamma_0^2}\right) .$$

$$(7.12)$$

Therefore, the error rate $P_{EPF}$ is determined by

$$P_{EPF} = \int_0^\infty dR_1 \int_{R_1}^\infty dR_2 \; p(R_1, R_2 \mid b_k = 1) \; , \tag{7.13}$$

or

$$P_{EPF} = prob\left(\frac{R_1}{R_2} < 1 \mid b_k = 1\right) , \tag{7.14}$$

under the assumption of the equally likely occurrence of "0" and "1". The substitution of (7.12) into either (7.13) or (7.14) leads to the derivation of the final result as

$$P_{EPF} = \frac{1}{2} - \frac{\rho_0 \rho_X(T)}{2(1+\rho_0)} \; . \tag{7.15}$$

This is consistent with the result obtained by Voelker [24], where the error rate of Differential Phase Shift Keying (DPSK) is discussed in the fast Rayleigh fading environments.

The calculation of the error rates necessitates the specification of $S_X(f)$ and $S_\xi(f)$. When a vehicle with a vertical monopole antenna is moving constantly through the multipath propagation field consisting of a large number of uniform plane waves, the power spectrum $S_X(f)$ is given by Gans [69]:

$$S_X(f) = \begin{cases} \dfrac{\sigma_c^2}{\pi\sqrt{f_D^2 - f^2}} \;, & |f| < f_D \\[2em] 0 \quad , & \text{otherwise} , \end{cases} \tag{7.16}$$

where $f_D$ is the maximum Doppler frequency. The normalized autocorrelation function $\rho_X(T)$ is obtained by performing the

inverse Fourier transformation of (7.16);

$$\rho_\chi(T) = J_0(2\pi f_D T) ,$$

<div align="right">(7.17)</div>

where $J_0(\cdot)$ is the zeroth order Bessel function of the first kind.

Assuming that $S_\xi(f)$ takes the form as

$$S_\xi(f) = \begin{cases} \dfrac{\sigma_n^2}{2B} , & |f| \leqq B \\[2em] 0 , & \text{otherwise,} \end{cases}$$

<div align="right">(7.18)</div>

the final results of the error rates can be derived by substituting (7.16)-(7.18) into (7.4) and (7.15):

$$P_{EFF} = \frac{1}{2}\left\{ 1 - \frac{\sqrt{2}\rho_\circ \Delta f_d/f_D}{\sqrt{(\rho_\circ+1)\{\rho_\circ[1+(\sqrt{2}\Delta f_d/f_D)^2]+(2B/\sqrt{6}f_D)^2\}}} \right\},$$

<div align="right">(7.19)</div>

$$P_{EPF} = \frac{1}{2}\left\{ 1 - \frac{\rho_\circ J_0(\pi f_D/\Delta f_d)}{1+\rho_\circ} \right\} . \qquad (\Delta f_d = \frac{1}{2T})$$

<div align="right">(7.20)</div>

When the Doppler effects may be neglected, that is, $f_D \longrightarrow 0$, the error rates (7.19) and (7.20) reduce to

$$P_{EFF} = \frac{1}{2}\left\{ 1 - \frac{\rho_\circ}{\sqrt{(\rho_\circ+1)\{\rho_\circ+(2B/2\sqrt{3}\Delta f_d)^2\}}} \right\},$$

<div align="right">(7.21)</div>

$$P_{EPF} = \frac{1}{2}\left\{ 1 - \frac{\rho_\circ}{1+\rho_\circ} \right\} .$$

<div align="right">(7.22)</div>

## 7.4  System Comparison

The system comparison is confined to the case of the time-selective fading, since the error rate characteristics for the nonselective fading is similar to those in Ch. 5.

One example of the numerical results is shown in Fig. 7.1 as functions of the maximum Doppler frequency to frequency deviation ratio $(f_D/\Delta f_d)$ and the average CNR $(\rho_o)$, when $2B=5\Delta f_d$. This figure shows the following results:

(1) In comparatively low $\rho_o$ regions, $P_{EPF}$ is slightly superior to $P_{EFF}$.

(2) In comparatively high $\rho_o$ regions, $P_{EFF}$ is much superior to $P_{EPF}$.

(3) The irreducible error rates are found and are dependent on the values of $f_D/\Delta f_d$ as given by

$$P_{EFF}|_{\rho_o \to \infty} = \frac{1}{2}[1- \frac{\sqrt{2}\Delta f_d/f_D}{\sqrt{1+(\sqrt{2}\Delta f_d/f_D)^2}}] , \qquad (7.23)$$

$$P_{EPF}|_{\rho_o \to \infty} = \frac{1}{2}[1-J_0(\pi f_D/\Delta f_d)] . \qquad (7.24)$$

(4) The Doppler phenomenon affects the phase information more strongly than the frequency information from the viewpoint of the error rate.

(5) When the Doppler effect is quite small or can be neglected $(f_D=0)$, $P_{EPF}$ is superior to $P_{EFF}$.
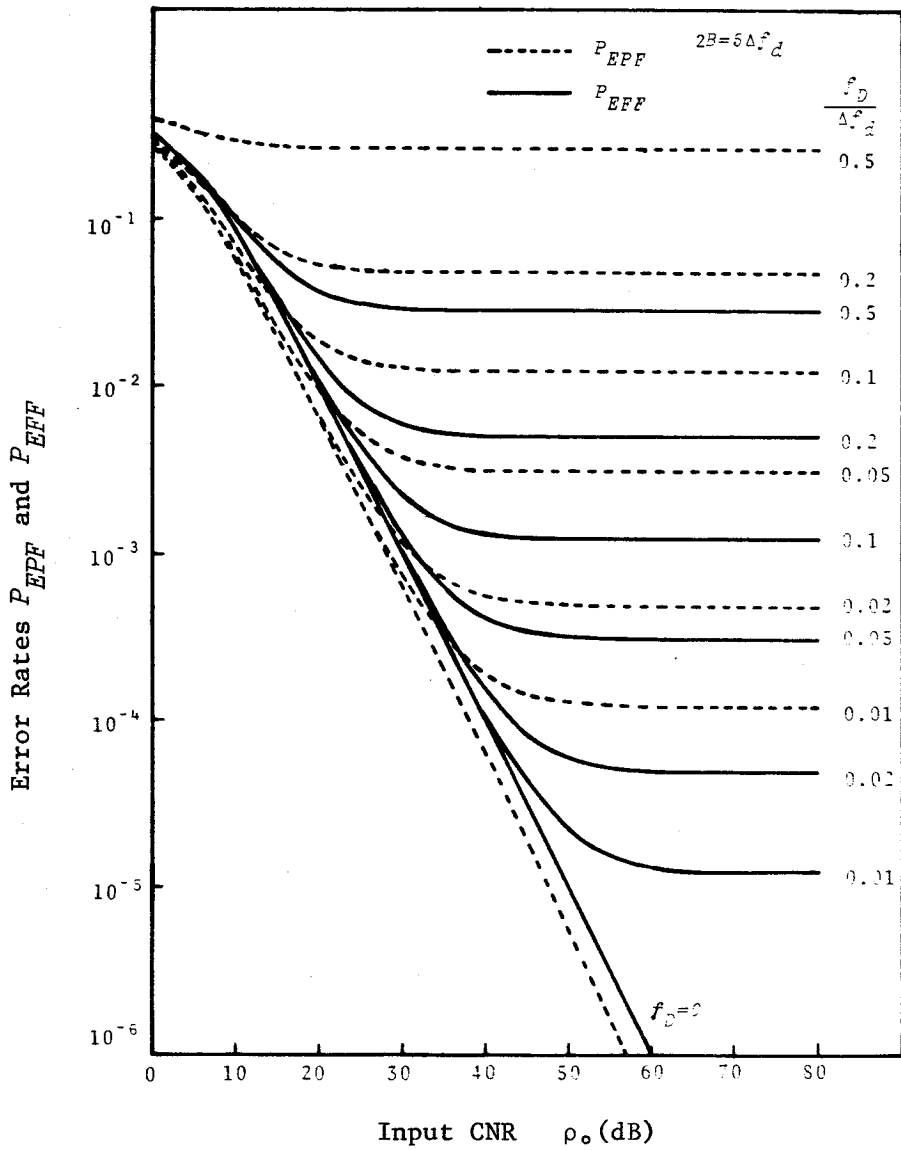
Fig. 7.1  Error Rates for Digital Phase-Frequency
Modulation Signal in Time-Selective Fading.

## 7.5 Concluding Remarks

In this chapter, the error rate characteristics of the PFSK signal has been discussed when applied to the land mobile radio communication system.  The main results are as follows:

(1) The Doppler phenomenon affects the phase information more strongly than the frequency information from the viewpoint of the error rate.

(2) When the Doppler effect can be neglected, the error rate for the phase information is superior to that for the frequency information.

# Chapter 8

## CONCLUSIONS

This work has theoretically investigated the detection characteristics of the analog frequency modulation, the digital frequency modulation, and the newly proposed digital phase-frequency modulation systms.

In order to discuss the detection characteristics in a wide class of fading environments, covering from deep to shallow fading environments, this work has adopted the $m$-distribution as the fading statistics. Especially, for the digital phase-frequency modulation system, the time-selective Rayleigh fading has been assumed in consideration of the application to the mobile radio communication system. In addition, the improvement effects owing to the diversity techniques combatting the effect of fading have been discussed including the influence of the correlation between two diversity branches. From the results obtained, the system comparisons have been done. In this chapter, the main results obtained in the previous chapters are described:

  (1) The output noise and the output SNR characteristics of the analog FM system in the nonselective $m$-distributed fading environments have been investigated. Additionally, the improvement effects owing to the three kinds of predetection diversity technique have been discussed including the influence of the correlation between two diversity branches. The main results can be summarized as follows:

(a) From the numerical results of the power ratio of
    click noise to random noise, it has been clarified
    that the fading affects the click noise more strongly
    than the random noise and that much more diversity
    improvement effects can be obtained for the click
    noise than for the random noise.

(b) From the numerical results of the output SNR, it has
    been shown that Maximal-Ratio Combining system has
    the largest improvement effects and that better out-
    put SNR performance can be obtained with smaller
    correlation coefficient between two diversity
    branches.

(2) The error rate characteristics of the FSK system in the
    nonselective $m$-distributed fading environments have been
    investigated. Additionally, the improvement effects
    owing to the four kinds of predetection diversity tech-
    nique and to the postdetection diversity technique have
    been discussed including the influence of the correlation
    between two diversity branches. In the case of Switch-
    and-Stay diversity, a design method of an optimum
    switching level attaining a minimum error rate has been
    described. The main results can be summarized as follows:

(a) The optimum modulation index yielding the minimum
    error rate is found and this index is not affected,
    except for the postdetection diversity, by the types of
    diversity, the average input CNR, the fading figure,
    and the correlation coefficient.

(b) The better branch dominates the error rate for the
    predetection diversity. On the other hand, the
    worse branch dominates that for the postdetection
    diversity.

(3) A digital phase-frequency modulation signaling by the combination of phase and frequency shift keyings has been newly proposed, and its detection systems and power spectral density have been discussed. Additionally, the error rate characteristics of this signal in the time-selective Rayleigh fading environments have been investigated. From the numerical results, it has been clarified that the Doppler phenomenon affects the phase information more strongly than the frequency information.

# Appendix A

## Table of Formulas [70]-[71]

$$\Gamma(s) = 2 \int_0^\infty e^{-t^2} t^{2s-1} \, dt \qquad\qquad (A.1)$$

$$\operatorname{erf}(x) = 1 - \operatorname{erfc}(x) \qquad\qquad (A.2)$$

$$\operatorname{erf}(x) = \frac{2x}{\sqrt{\pi}} \, {}_1F_1\left(\frac{1}{2}; \frac{3}{2}; -x^2\right) \qquad\qquad (A.3)$$

$$ {}_1F_1(a; b; -z) = e^{-z} \, {}_1F_1(b-a; b; z) \qquad\qquad (A.4)$$

$$g(p) = \int_0^\infty e^{-pt} f(t) \, dt \qquad\qquad (A.5)$$

$$f(t) = t^{\sigma-1} \, {}_mF_n(a_1 \cdots a_m; \rho_1 \cdots \rho_n; \lambda t)$$

$$g(p) = \Gamma(\sigma) \, {}_{m+1}F_n(a_1 \cdots a_m, \sigma; \rho_1 \cdots \rho_n; \lambda/p)$$

$$\int_0^\infty t I_0(\alpha t) e^{-(t^2+\alpha^2)/2} \, dt = 1 \qquad\qquad (A.6)$$

# Appendix B

## Derivation of $N_{O\dot{y}}$

The power spectral density $S_y(f)$ is given by

$$S_y(f) = S_\xi(f) \otimes S_L(f) \ , \tag{B.1}$$

where "$\otimes$" denotes the frequency convolution, and

$$S_\xi(f) = \begin{cases} \dfrac{\sigma_n^2}{2B} \ , & |f| \le B \\ \\ 0 \ , & \text{otherewise.} \end{cases} \tag{B.2}$$

Therefore, $S_y(f)$ can be calculated as follows:

$$S_y(f) = \frac{\sigma_n^2}{8\beta r^2 f_m} \left\{ \mathrm{erf}(\sqrt{2} + \frac{f}{\sqrt{2}\beta f_m}) + \mathrm{erf}(\ 2 - \frac{f}{\sqrt{2}\beta f_m}) \right\} \ . \tag{B.3}$$

When $\beta \ge 5$, the random noise power $N_{O\dot{y}}$ becomes approximately

$$N_{O\dot{y}} = \int_{-f_m}^{f_m} 4\pi^2 f^2 S_y(f) df$$

$$\simeq \frac{1}{r^2} \cdot \frac{2\pi^2 \sigma_n^2 f_m^2 \mathrm{erf}(\sqrt{2})}{3\beta} \ . \tag{B.4}$$

# Appendix  C

## Derivation of $M_o^2$

The variance $E[\overset{\bullet}{a}_o^2]$ is given by

$$E[\overset{\bullet}{a}_o^2]= \int_{-\infty}^{\infty} (2\pi f)^2 S_\xi(f)\,|H(f)|^2 df \ , \qquad (C.1)$$

where $H(f)$ is the Fourier transformation of $h(\tau)$ in (4.6),

$$H(f)= \int_{-\infty}^{\infty} h(\tau)e^{-j2\pi f\tau}d\tau$$

$$= \frac{\sin(\pi fT)}{\pi fT} \ , \qquad (C.2)$$

$$S_\xi(f)= \begin{cases} \dfrac{\sigma_n^2}{2B} \ , & |f| \le B \\[2ex] 0 \ , & \text{otherwise,} \end{cases} \qquad (C.3)$$

and $2B$ is the bandwidth of the input bandpass filter, which is related to digit duration $T$ and modulation index $\beta$ as

$$2B=2(\beta+1)\frac{1}{2T} \ , \qquad (C.4)$$

$$\beta=\Delta\omega_d T/\pi \ . \qquad (C.5)$$

Therefore, $M_o^2$ can be calculated as follows:

$$M_o^2= \frac{E[a_o^2]}{r^2}=\frac{2\sigma_n^2 f_o(\beta)}{r^2 T^2} \ , \qquad (C.6)$$

where

$$f_o(\beta)=1-\frac{\sin\pi(\beta+1)}{\pi(\beta+1)} \ . \qquad (C.7)$$

# References

[1] D.Middleton, *Statistical Communication Theory*. New York: McGraw-Hill, 1960.

[2] H. E. Rowe, *Signals and Noise in Communication Systems*. Princeton: Van Nostrand, 1965.

[3] W. R. Bennett and J. R. Davey, *Data Transmission*. New York: McGraw-Hill, 1965.

[4] M. Schwartz, W. R. Bennett, and S. Stein, *Communication Systems and Techniques*. New York: McGraw-Hill, 1966.

[5] E. D. Sunde, *Communication Systems Engineering Theory*. New York: Wiley, 1969.

[6] H. Taub and D. L. Schilling, *Principles of Communication Systems*. New York: McGraw-Hill, 1971.

[7] J. E. Miller, "ATS-6 Television Relay Using Small Terminals Experiment," *IEEE Trans. Aeros. Electron. Syst.*, vol. AES-11, pp. 1038-1047, Nov. 1975.

[8] K. M. Uglow, "Multiplex Telemetry Modulation and Demodulation Methods," *IEEE Trans. Commun. Technol.*, vol. COM-16, Feb. 1968.

[9] C. C. Pfitzer and S. A. Leslie, "Methods of Determining Paging Receiver in a Multiple Transmitter Environment," in *Conf. Rec., 1975 IEEE Int. Conf. Commun.*, San Francisco, Ca., pp.37.25-37.29.

[10] S. Komaki, I. Horikawa, K. Morita, and Y. Okamoto, "Characteristics of a High Capacity 16 QAM Digital Radio Systems in Multipath Fading," *IEEE Trans. Commun.*, vol. COM-27, pp. 1854-1861, Dec. 1979.

[11] C. Chayavadhanangkur and J. H. Park, Jr., "Analysis of FM Systems with Co-Channel Interference Using a Click Model," *IEEE Trans. Commun.* vol. COM-24, pp. 903-910, Aug. 1976.

[12] J. H. Park, Jr., "Effect of Fading on FM Reception with Cochannel Interference," *IEEE Trans. Aerosp. Electron. Syst.*, vol. AES-13, pp. 127-132, March 1977.

[13] T. Mizutani, K. Kashiki, N. Morinaga, and T. Namekawa, "Effects of Interference on FSK Signal," *Paper of Technical Group on Communication Systems, IECE of Japan,* CS79-39, May 1979 (in Japanese).

[14] T. Mizutani, K. Kashiki, N. Morinaga, and T. Namekawa, "Effects of Interference on FSK Signal [II]," *Proceeding of the 2nd Symposium on Information and Its Applications,* pp. 141-148. Nov. 1979 (in Japanese).

[15] T. Mizutani, K. Kashiki, N. Morinaga, and T. Namekawa, "Interference Characteristics of Analog FM Signal on Digital FM Signal," *1980 Nat. Conf. Rec. on Communication Engineering,IECE of Japan,* no. 470, Sept. 1980 (in Japanese).

[16] T. Mizutani, K. Kashiki, N. Morinaga, and T. Namekawa, "Effects of Interference on FSK Signal [III]," *Paper of Technical Group on Communication Systems, IECE of Japan,* CS80-176, pp. 25-30, Dec. 1980 (in Japanese).

[17] H. E. Rowe, "Frequency or Phase Modulation with a Noise Carrier," *Proc. IEEE,* vol. 52, pp. 396-408, April 1964.

[18] D. L. Schilling, E. A. Nelson, and K. K. Clarke, "Discriminator Response to an FM Signal in a Fading Channel," *IEEE Trans. Commun. Technol.,* vol. COM-15, pp.252-263, April 1967.

[19] G. L. Turin, "The Effect of Fading on the Output Spectrum of an FM System," *IEEE Trans. Inform. Theory*, vol. IT-14, pp. 265-267, March 1968.

[20] B. R. Davis, "FM Noise with Fading Channels and Diversity," *IEEE Trans. Commun. Technol.*, vol. COM-19, pp. 1189-1200, Dec. 1971.

[21] R. S. Kennedy, *Fading Dispersive Communication Channels*, New York: Wiley, 1969.

[22] M. Nakagami, "The m-distribution — A General Formula of Intensity Distribution of Rapid Fading," in *Statistical Methods in Radio Waves Propagation*, W. C. Hoffman Ed. New York: Pergamon, 1960, pp. 3-36.

[23] W. C. Jakes, Jr., *Microwave Mobile Communications*, John Wiley and Sons Inc., New York, 1974.

[24] H. Voelcker, "Phase-Shift-Keying in Fading Channels," *Proc. IEE*, vol. 107, part B, pp. 31-38, Jan. 1960.

[25] K. Hirade, M. Ishizuka, and F. Adachi, "Error-Rate Performance of Digital FM with Discriminator-Detection under Fast Rayleigh Fading Environment," *Trans. IECE of Japan*, vol. 61-E, pp. 704-709, Sept. 1978.

[26] K. Hirade, M. Ishizuka, F. Adachi, and K. Ohtani, "Error-Rate Performance of Digital FM with Differential Detection in Land Mobile Radio Channels," *IEEE Trans. Veh. Technol.*, vol. VT-28, pp. 204-212, Aug. 1979.

[27] D. G. Brennan, "Linear Diversity Combining Techniques," *Proc. IRE*, vol. 47, pp. 1075-1102, June 1959.

[28] M. J. Gans, "The Effect of Gaussian Error in Maximal Ratio Combiners," *IEEE Trans. Commun. Technol.*, vol. COM-19, pp. 492-500, Aug. 1971.

[29] P. Prapinmongkolkarn, N. Morinaga, and T. Namekawa, "Performance of Digital FM Systems in a Fading Environment," *IEEE Trans. Aerosp. Electron. Syst.*, vol. AES-10, pp.698-709, Sept. 1974.

[30] Y. Miyagaki, N. Morinaga, and T. Namekawa, "Error Probability Characteristics for CPSK Signal Through m-Distributed Fading Channel," *IEEE Trans. Commun.*, vol. COM-26, pp. 88-100, Jan. 1978.

[31] S. O. Rice, "Noise in FM Receivers," in *Time Series Analysis*, M. Rosenblatt, Ed. New York: Wiley, 1963, Ch. 25, pp. 395-422.

[32] J. Cohn, "A New Approach to the Analysis of FM Threshold Reception," *Proc. Nat. Electronics Conf.*, vol. 12, pp. 221-236, 1956.

[33] W. H. Lob, "The Distribution of FM-Discriminator Click Widths," *Proc. IEEE*, vol. 57, pp. 732-733, April 1969.

[34] M. Ejiri, T. Onodera, T. Takahashi, and Y. Enami, "Visual Effect of Impulsive Noise and Its Weighting in Television Systems," *J. Inst. TV Engrs. of Japan*, vol-31, pp. 870-875, Nov. 1977.

[35] W. R. Bennet and J. Salz, "Binary Data Transmission by FM over a Real Channel," *Bell Sys. Tech. J.*, vol. 42, pp. 2387-2426, Sept. 1963.

[36] P. D. Shaft, "Error Rate of PCM-FM using Discriminator Detection," *IEEE Trans. Space Electron. Telem.*, vol. SET-9, pp. 131-137, Dec. 1963.

[37] G. F. Montgomery, "A Comparison of Amplitude and Angle Modulation for Narrowband Communication of Binary-Coded Message in Fluctuation Noise," *Proc. IRE*, vol. 42, pp. 447-454, Feb. 1954.

[38] J. Salz and S. Stein, "Distribution of Instantaneous Frequency for Signal plus Noise," *IEEE Trans. Inform. Theory*, vol. IT-10, pp.272-274, Oct. 1964.

[39] S. O. Rice, "Statistical Properties of a Sine Wave plus Random Noise," *Bell Sys. Tech. J.*, vol.27, pp. 109-151, Jan. 1948.

[40] D. L. Schilling, E. Hoffman, and E. A. Nelson,"Error
Rates for Digital Signals Demodulated by an FM Discrimi-
nator," *IEEE Trans. Commun. Technol.*, vol. COM-15, pp.
507-517, Aug. 1967.

[41] D. L. Schilling and I. Ringdahl, "On the Distribution of
Spikes seen at the Output of an FM Discriminator below
Threshold Reception," *Proc. IEEE*, vol. 52, pp.1756-1757,
Dec. 1964.

[42] D. Yavuz and D. T. Hess, "FM Noise and Clicks," *IEEE
Trans. Commun. Technol.*, vol. COM-17, pp. 648-653, Dec.
1969.

[43] A. Papoulis, *Probability, Random Variables, and Stochas-
tic Processes*. New York: McGraw-Hill, 1965.

[44] W. B. Davenport and W. L. Root, *An Introduction to the
Theory of Random Signals and Noise*. New York: McGraw-
Hill, 1958.

[45] K. Kashiki, N. Morinaga, and T. Namekawa,"Signal-to-Noise
Ratios in Fading FM Communication Systems and Improve-
ment Effects by Diversity Reception," *Paper of Technical
Group on Communication Systems, IECE of Japan,* CS76-90,
pp. 33-40, Aug. 1976 (in Japanese).

[46] K. Kashiki, N. Morinaga, and T. Namekawa, "FM Noise
Characteristics in Fading Communication Systems," *Paper
of Image Transmission Research Committee Meeting, Inst.
TV Engrs. of Japan,* IT22-9, Sept. 1976 (in Japanese).

[47] K. Kashiki, N. Morinaga, and T. Namekawa, "Output Signal-
to-Noise Power Ratio Characteristics in FM Communication
Systems with Fading," *J. Inst. TV Engrs. of Japan,* vol.
32, pp. 686-692, Aug. 1978 (in Japanese).

[48] S. Stein and J. J. Jones, *Modern Communication Principles*.
New York: McGraw-Hill, 1967.

[49] P. D. Shaft, "On the Relationship between Scintillation Index and Rician Fading," *IEEE Trans. Commun.*, vol. COM-22, pp.731-732, May 1974.

[50] Y. Miyagaki, N. Morinaga, and T. Namekawa, " Improvement by Diversity Reception in Fading PSK Communication Channel," *Trans. IECE of Japan*, vol. 58-B, pp. 441-448, Sept. 1975 (in Japanese).

[51] J. Klapper, "Demodulation Threshold Performance and Error Rates in Angle Modulated Digital Signals," *RCA Rev.*, vol. 27, pp. 226-244, June 1966.

[52] J. E. Mazo and J. Salz, "Theory of Error Rates for Digital FM," *Bell Sys. Tech. J.*, vol. 45, pp. 1511-1535, Nov. 1966.

[53] W. K. Pratt, *Laser Communication Systems*, New York: Wiley, 1969, pp. 257-258.

[54] J. Hancock and P.Wintz, *Signal Detection Theory*. New York: McGraw-Hill, 1966.

[55] K. Kashiki, N. Morinaga, and T. Namekawa, "Error Rates and Diversity Effects for Fading FSK Signal," *Paper of Technical Group on Communication Systems, IECE of Japan*, CS76-167, pp. 51-58, Jan. 1977 (in Japanese).

[56] K. Kashiki, N. Morinaga, and T. Namekawa, "Post-Detection Diversity Improvements for Fading FSK Signal," *Paper of Technical Group on Communication Systems, IECE of Japan*, CS78-101, pp. 47-54, Aug. 1978 (in Japanese).

[57] K. Kashiki, N. Morinaga, and T. Namekawa, "An Optimum Switching Level for Switch and Stay Diversity Techniques," to be published in *Trans. IECE of Japan, (B)*, (in Japanese).

[58] E. A. Nelson and D. L. Schilling, "Response of an FM Discriminator to a Digital FM Signal in Randomly Fading Channels," *IEEE Trans. Commun., Technol.*, vol. COM-16, pp. 551-560, Aug. 1968.

[59] A. J. Rustako, Jr., Y. S. Yeh, and R. R. Murray,"Perfor-
     mance of Feedback and Switch Space Diversity 900 MHz FM
     Mobile Radio Systems with Rayleigh Fading," *IEEE Trans.
     Commun.*, vol. COM-21, pp. 1257-1268, Nov. 1973.

[60] F. Adachi and T. Hattori, "Postdetection Diversity Effect
     in a Digital FM Land Mobile Radio," *Trans. IECE of Japan*,
     vol. J63-B, PP. 349-356, April 1980 (in Japanese).

[61] F. Adachi, "Postdetection Selection Diversity Effects in
     a Digital FM Land Mobile Radio with Discriminator and
     Differential Detections," *Trans. IECE of Japan*, vol.
     J63-B, pp. 759-766, Aug. 1980 (in Japanese).

[62] K. Kashiki, N. Morinaga, T. Namekawa, "A Consideration
     on Noncoherent Detection Methods of Digital Phase-
     Frequency Modulation Signal," *Paper of Technical Group
     on Communication Systems, IECE of Japan*, CS79-237,
     pp. 17-20, Feb. 1980 (in Japanese).

[63] C. R. Cahn, "Combined Digital Phase and Amplitude Modu-
     lation Communications," *IRE Trans. Commun. Syst.*, vol.
     CS-8, pp. 150-155, Sept. 1960.

[64] J. C. Hancock and R. W. Lucky, "Performance of Combined
     Amplitude and Phase-Modulated Communication Systems,"
     *IRE Trans. Commun. Syst.*, vol. CS-8, pp. 232-237, Dec.
     1960.

[65] J. Salz, J. R. Sheehan, and D. J. Paris, "Data Trans-
     mission by Combined AM and PM," *Bell Syst. Tech. J.*,
     vol. 50, pp. 2399-2419, Sept. 1971.

[66] G. R. Welti, "Application of Hybrid Modulation to FDMA
     Telephony via Satellite," *COMSAT Tech. Rev.*, vol. 3,
     pp. 419-429, Fall 1971.

[67] G. J. Foschini, R. D. Gitlin and S.B. Weinstein, "On the
     Selection of a Two-Dimensional Signal Constellation in
     the Presence of Phase Jitter and Gaussian Noise," *Bell
     Syst. Tech. J.*, vol. 52, pp. 927-965, July-Aug. 1973.

[68] C.M. Thomas, M. Y. Weinder, and S. H. Durrani, "Digital Amplitude-Phase Keying with *M*-ary Alphabets," *IEEE Trans. Commun.*, vol. COM-22, Feb. 1974.

[69] M. J. Gans, "A Power Spectral Theory of Propagation in the Mobile-Radio Environment," *IEEE Trans. Veh. Technol.* vol. VT-21, pp.27-38, Feb. 1972.

[70] S. Moriguchi, K. Udagawa, and S. Hitotsumatsu, *Mathematical Formulas (III)*. Tokyo: Iwanamishinsho,1960.

[71] I.S. Gradshteyn, I. M. Ryzhik, *Table of Integrals, Series, and Products*. New York: Academic Press,1965.